YEDITEPE UNIVERSITY
INSTITUTE OF HEALTH SCIENCES
DEPARTMENT OF PHARMACEUTICAL SCIENCES

NOVEL ANTICANCER THIAZOLIDINE MOLECULES: DESIGN, SYNTHESIS AND EVALUATION

MASTER of SCIENCES THESIS

KEREM BURAN

ISTANBUL - 2013

NOVEL ANTICANCER THIAZOLIDINE MOLECULES: DESIGN, SYNTHESIS AND EVALUATION

A THESIS SUBMITTED TO YEDITEPE UNIVERSITY
THE GRADUATE SCHOOL OF HEALTH SCIENCES
IN PARTIAL FULFILLMENT OF THE REQUIREMENTS FOR
THE DEGREE OF MASTER OF SCIENCE
IN
PHARMACEUTICAL CHEMISTRY

BY
KEREM BURAN

SUPERVISOR
Ass. Prof. Dr. FİLİZ ESRA ÖNEN BAYRAM

ISTANBUL - 2013

Yüksek Lisans (Master) öğrencisi Kerem Buran'ın çalışması jürimiz tarafından Farmasötik Kimya Anabilim Dalı Master tezi olarak uygun görülmüştür.

İMZA

Başkan : Prof. Dr. Hülya AKGÜN
Üniversite : Yeditepe Üniversitesi

Üye : Prof. Dr. Fethi ŞAHİN
Üniversite : Doğu Akdeniz Üniversitesi

Üye : Prof. Dr. Mine Yarım YÜKSEL
Üniversite : Yeditepe Üniversitesi

Üye : Doç. Dr. Meriç Köksal AKKOÇ
Üniversite : Yeditepe Üniversitesi

Üye : Yard. Doç Dr. F.Esra Önen BAYRAM
Üniversite : Yeditepe Üniversitesi

ONAY

Yukarıdaki jüri kararı Enstitü Yönetim Kurulu'nun 25/12/2013 tarih ve 17/5 sayılı kararı ile onaylanmıştır.

Prof. Dr. Bayram YILMAZ
Müdür

ÖZET

BURAN, K. Antikanser özelliği olan yeni tiyazolidin moleküllerinin: tasarım, sentez ve değerlendirmeleri. Yeditepe Üniversitesi, Sağlık Bilimleri Enstitüsü Farmasötik Kimya Programı Bilim Uzmanlığı Tezi, İstanbul 2013.

Kanser, normal vücut hücrelerinin düzensiz bir şekilde büyümesi sonucu oluşan bir hastalıktır. Günümüzde kanser tedavileri çeşitlilik göstermekle beraber, klasik tedavi metotlarında kanserli hücrelerde apoptozun (programlı hücre ölümü) tekrar aktive edilmesi yaygın olarak kullanılan bir tedavi stratejisidir. Buna göre yapılan yeni anti-kanser molekül tasarım çalışmalarında moleküllerin apoptoz tetikleyici etkisinin olması hedeflenen özellikler arasındadır. Bu bağlamda, (*2RS,4R*)-2-fenil-3-propiyonil-tiyazolidin-4-karboksilik asit etil ester (ALC67) molekülünün anti-kanser ve apoptoz tetikleyici özelliği olduğu kısa zaman önce belirtilmiştir. Çalışmamızda ALC67 molekülünün 2 pozisyonunda bulunan fenil halkasının aktivite üzerindeki etkisini araştırmak adına halka, aromatik ve alifatik gruplarla değiştirilerek on bir türev (**3a-3m**) sentezlenmiştir.

ALC67 molekülünün yeni türevleri üç basamakta sentezlenmiş olup; birinci basamakta, *L*-sistein ve aldehit kullanılarak tiyazolidin halka yapısı oluşturulmuştur (**1a-1m**). Sonrasında, sentezlenen tiyazolidin halkasına, etil ester grubu (**2a-2m**) ve propiyonil grubu (**3a-3m**) bağlanarak türevlendirilmiştir. Bu çalışmada otuz üç yeni molekül sentezlenip, sentezlenen moleküllerin çoğunluğunun yapıları FT-IR, ^{1}H NMR, ^{13}C NMR ve LC-MS ile aydınlatılmıştır.

Yeni sentezlenen (2RS,4R)-2-fenil-3-propiyonil-tiyazolidin-4-kaboksilik asit etil ester yapısının türevleri olan maddelerin (**3a-3m**) sitotoksik aktivite testleri insan karaciğer kanser hücre hatları (HUH7 ve Mahlavu) üzerinde sulforodamin B (SRB) yöntemi kullanılarak yapılmıştır. Elde edilen test sonuçlarına göre, fenil grubunun değişmesi sitotoksik aktiviteyi değiştirmemiştir.

Sonuç olarak, yaptığımız bu çalışmamızda yeni tiyazolidin türevlerinin anti-kanser etkisi olduğu gösterilmiş ve anti-kanser özellik gösteren yeni bir tiyazolidin sınıfı geliştirilmiştir.

Anahtar kelimeler: Tiyazolidin, terminal alkin, antikanser, apoptoz.

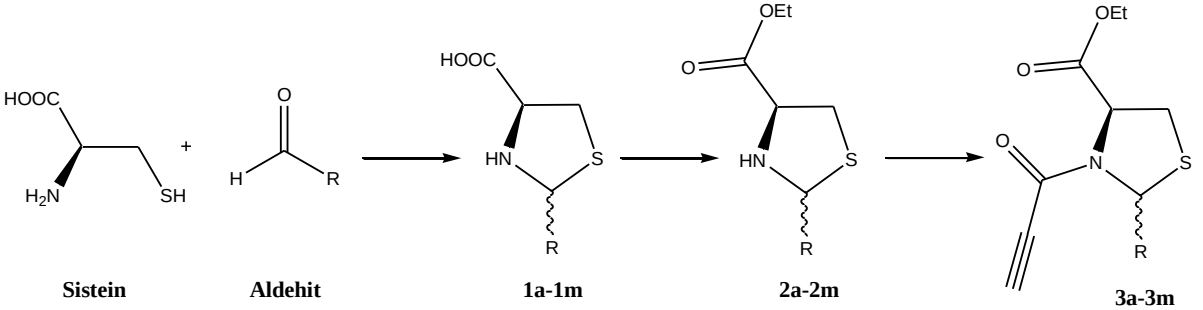

Sistein **Aldehit** **1a-1m** **2a-2m** **3a-3m**

ABSTRACT

BURAN, K. Novel anticancer thiazolidine molecules: design, synthesis and evaluation. Yeditepe University Institute of Health Science, Thesis on Pharmaceutical Chemistry Master of Science Degree Programme, Istanbul, 2013.

Cancer results from unregulated cell growth. Reactivating cell death in cancer cells, i.e. apoptosis, is a classical anticancer therapeutic strategy. The apoptosis-inducer property of the (*2RS,4R*)-2-phenyl-3-propinoyl-thiazolidine-4-carboxylic acid ethyl ester (ALC67) molecule has been discovered recently. To elucidate the mechanism of action of this molecule and to evaluate the impact of the phenyl group that the thiazolidine ring presents at its second position on the cytotoxicity, we developed eleven ALC 67 analogues (**3a-3m**) replacing the phenyl moiety with various aliphatic and aromatic groups.

The synthesis of ALC67 analogues required three major steps. The first step consisted of the formation of the thiazolidine ring using *L*-cysteine and an aldehyde (**1a-1m**). Then, the thiazolidine ring was modified in order to first introduce the ethyl ester moiety (**2a-2m**) and then the propionyl group (**3a-3m**). A total of thirty three novel molecules were obtained and most of compounds were characterized by FT-IR, ^{1}H NMR, ^{13}C NMR and LC-MS.

The cytotoxic activity of the novel (*2RS,4R*)-2-phenyl-3-propinoyl-thiazolidine-4-carboxylic acid ethyl ester derivatives (**3a-3m**) were evaluated on human liver HUH7 and Mahlavu hepatocellular carcinoma cell (HCC) lines with the sulforhodamine B (SRB) assay. Results demonstrated that the antiproliferative property was conserved when the phenyl moiety was replaced.

Thus, with this investigation a novel class of thiazolidine derivatives with promising anticancer activity was developed.

Keywords: Thiazolidine, terminal alkyne, anticancer, apoptosis.

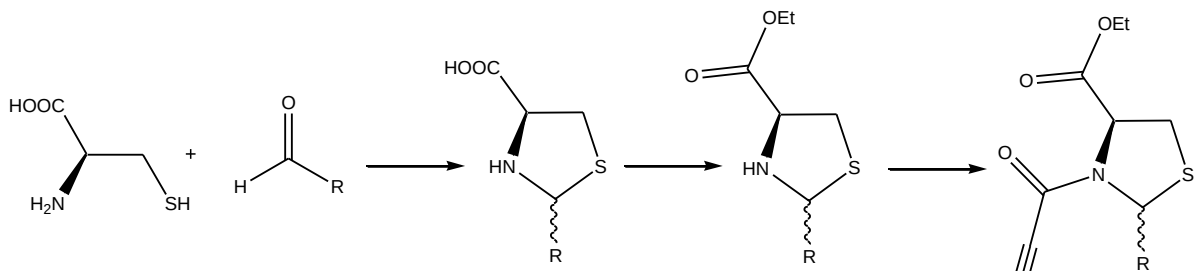

Cysteine **Aldehyde** **1a-1m** **2a-2m** **3a-3m**

to the memory of Prof. Dr. Ayhan S. Demir…

ACKNOWLEDGEMENTS

I would like to present my gratitude to my supervisor Ass. Prof. Dr. Filiz Esra Önen Bayram for being such great mentor and guiding me with a great patience.

I would like to present my gratitude to Dean of Faculty of Pharmacy at Yeditepe University Prof. Dr. Hülya Akgün for her support in all aspects.

I would like to express my sincere appreciation to Prof. Dr. Ayhan S. Demir.

I would like to thank Assoc. Prof. Dr. Rengül Çetin Atalay and M.Sci. İrem Durmaz at Bilkent University, Faculty of Science, Department of Molecular Biology and Genetics for activity tests studies.

I would like to thank to Prof. Dr. Hakan Göker at Ankara University, Faculty of Pharmacy, Department of Pharmaceutical Chemistry for ^{1}H NMR, ^{13}C NMR and LC-MS analyses.

I would like to thank to all the academic staff at Pharmaceutical Chemistry Department of Yeditepe University for their valuable contribution for every respect.

I also would like to express my deep gratitude to Ass. Prof. Dr. Hayati Çelik for his guidance, advice and sharing his personal experience.

I would like to thank my friends and colleagues Miralem Jakirlic, Dr. Mehmet Göllü and Reyhan Kahveci Ulugöl for their help, friendship and advice.

I would like to extend my gratitude to Ass. Prof. Dr. Mustafa Emrullahoğlu at İzmir Yüksek Teknoloji Enstitüsü.

Finally, my special appreciation and great gratitude is devoted to my parents and my brother Eren for their love, encouragement and patience.

TABLE of CONTENTS

ÖZET	ii
ABSTRACT	iii
DEDICATION	iv
ACKNOWLEDGEMENTS	v
TABLE of CONTENTS	vi
ABBREVIATIONS	ix
TABLE of FIGURES	xi
TABLE of SCHEMES	xii
TABLE of TABLES	xiii

TABLE OF CONTENTS

1 INTRODUCTION AND AIM 1

2 GENERAL INFORMATION 3

2.1 Development of cancer 3

2.2 Thiazolidines: Synthesis and NMR characterization 7

2.2.1 Synthesis 7

2.2.2 ^{1}H NMR characterization 8

2.2.3 ^{13}C NMR characterization 11

2.3 Thiazolidines as anticancer agents 12

2.3.1 Thiazolidines anticancer property derives from thiazolidinones' activity 12

2.3.2 First antiproliferative thiazolidines: 2-arylthiazolidine-4-carboxylic acid amides (ATCAAs) 14

2.3.3 ALC67: An apoptotic thiazolidine derivative 17

2.3.4 [Indoline-3,2'-thiazolidine]-based apoptotic compounds 18

2.4 ALC67 derivatives: Development of novel antiproliferative thiazolidine compounds 20

3 MATERIALS AND METHODS 21

3.1 Chemicals 21

3.2 Synthetic Procedures 21

3.2.1 General procedure for **1a**-**1m**: 21

3.2.2 General Procedure for **2a**-**2m**: 21

3.2.3 General Procedure for **3a**-**3m**: 21

3.3 Analytical Methods 22

3.3.1 Controls by Thin Layer Chromatography (TLC) solvent systems 22

3.3.2 Spectrometric Analyses 23

3.3.2.1 Infrared Spectra: 23

3.3.2.2 ^{1}H-NMR Spectra: 23

3.3.2.3 ^{13}C-NMR Spectra: 23

3.3.2.4 LC-MS Spectra: 23

3.4 Activity Test Procedure: Sulforhodamine B Assay 23

4 EXPERIMENTAL 24

4.1 Spectral data for **1a - 1m**: 24
4.2 Data for **2a** – **2m** 36
4.3 Spectral data for **3a** – **3m** 43
5 RESULTS AND DISCUSSION 54
5.1 Chemistry 54
5.1.1 Generation of the thiazolidine cycle: synthesis of **1a-1m** 54
5.1.2 The esterification step: Synthesis of **2a**-**2m** 58
5.1.3 Acylation of the heterocyclic secondary amine: Synthesis of **3a**-**3m** 60
5.2 Biology 63
6 CONCLUSION 66
7 REFERENCES 67

ABBREVIATIONS

ALC67	(*2RS, 4R*)-2-phenyl-3-propinoyl-thiazolidine-4-carboxylic acid ethyl ester
aq	Aqueous
ATCAA	2-arylthiazolidin-4-carboxylic acid amide
COX	Cyclooxygenase
d	Doublet
DCC	N-N'-Dicyclohexylcarbodiimide
DCM	Dichloromethane
dd	Doublet of doublet
DMSO	Dimethylsulfoxide
DNA	Deoxyribonucleic acid
EDC	N-(3-dimethylaminopropyl)-N'-ethylcarbodiimide
ELSD	Evaporative light scattering detector
EtOH	Ethanol
FT-IR	Fourier transform infrared
GF	Growth factor
HCC	Hepatocellular carcinoma
HOBt	Hydroxybenzotriazole
IC_{50}	The half maximal inhibitory concentration
LC-MS	Liquid chromatography-mass spectrometry
LPA	Lysophosphatidic acid
m	Multiplet
MDM2	Mouse double minute 2 homolog
MV	Mahlavu
NMR	Nuclear magnetic resonance
NOE	Nuclear overhauser effect
p.	Page
PBS	Phosphate buffered saline
PCD	Programmed cell death
PDGF	Platelet-derived growth factor

ppm	Parts-per-million
RT	Room temperature
rt	Retention time
s	Singlet
SAP	Serine amide phosphate
SRB	Suforhodamine B assay
t	Triplet
td	Triplet of doublet
TLC	Thin layer chromatography
TNFα	Tumor necrosis factor α
UV	Ultraviolet light
v/v	volume/volume
VEGF	Vascular endothelial growth factor
w/v	weight/volume

TABLE OF FIGURES

Figure 1. Mustard gases 1
Figure 2. Structure of the ALC67 molecule and its derivatives. 2
Figure 3. Hallmarks of cancer 3
Figure 4. Apoptosis: the programmed cell death process. 5
Figure 5. Extrinsic and intrinsic apoptotic pathways. 6
Figure 6. Leads thiazolidine formation to diastereomeric mixtures. 7
Figure 7. Possible pathways for the generation of a thiazolidine ring. 8
Figure 8. Typical ^{1}H NMR of thiazolidine rings obtained from acetalation of L-cysteine. 10
Figure 9. The characteristic ^{13}C NMR peaks of diastereomic mixture of thiazolidines. 11
Figure 10. Benzimidazole substituted phenylimino-4-thiazolidinone derivatives 12
Figure 11. Structures of LPA and SAP. 12
Figure 12. Structure of SAP and 4-thiazolidinone derivatives: 2-aryl-4-oxo-thiazolidin-3yl-amides 13
Figure 13. Structures of opened-ring compounds 15
Figure 14. The small-molecule library around the thiazolidine scaffold 17
Figure 15. Inhibition of p53-MDM2 interaction with spiro(oxindole-3,3'-thiazolidine) derivatives 19
Figure 16. Two inactive molecules that are structurally related to ALC 67 20
Figure 17. A. ^{1}H NMR of **1l**, B. ^{13}C NMR of **1l** 57
Figure 18. FT-IR spectra of **1k** and **2k** 59
Figure 19. Decomposition of ethyl ester derivatives with time 59
Figure 20. FT-IR spectrum of **3k** depicting the characteristic bands of the terminal alkyne function 61
Figure 21. NMR spectra of **3i** exhibiting characteristic peaks of the terminal alkyne function 62

TABLE OF SCHEMES

Scheme 1. Reagents and conditions for synthesis of SAPs derivatives 13
Scheme 2. Reagents and conditions for synthesis of thiazolidinone amides 14
Scheme 3. Synthetis of ATCAAs 15
Scheme 4. Preparation of ALC 67 17
Scheme 5. Retrosynthesis of (2RS,4R) 3-propionyl-thiazolidine-4-carboxylic acid ethyl ester ... 54
Scheme 6. Cyclisation of *L*-cysteine in basic conditions. 55
Scheme 7. Reaction mechanism of the conversion of carboxylic acid derivatives into ethyl esters. 58
Scheme 8. Mechanism of the DCC activated peptidic coupling reaction. 60
Scheme 9. Synthetic pathway for the introduction of BODIPY to ALC67 66

TABLE OF TABLES

Table 1. IC_{50} values of ATCAA derivatives on melanoma and prostate cancer cell lines.....16
Table 2. IC_{50} values of ALC 67 in liver, breast, colon, and endometrial cancer cell lines. 18
Table 3. IC_{50} values of indoline-thiazolidine derivatives on MCF7 and HT29 cancer cell lines. ..19
Table 4. Yields of (*2RS,4R*)-2-Phenylthiazolidine-4-carboxylic acids **1a**-**1m** 56
Table 5. Yields of **3a-3m.** 63
Table 6. IC_{50} values of ALC67 analogues on HUH7 and Mahlavu (MV) hepatocellular carcinoma cell lines determined by the SRB assay. 64

1 INTRODUCTION AND AIM

Cancer is a term used for diseases in which abnormal cells divide without control and are able to invade other tissues. Cancer has probably existed since the origin of mankind; therefore, several ways of cancer treatment have been investigated. Nowadays, chemotherapy is one of the most important treatment methods for cancer. This has led to the investigation and development of cytotoxic drugs (chemotherapeutic agents).

The history of chemotherapeutic agents started with mustard gas (bis(2-chloroethyl)sulfide) (Figure 1, A) during World War I, it was used as a chemical weapon. However, autopsies performed on the victims' bodies revealed that lymphoid and myeloid suppression had taken place.

This led to the hypothesis that mustard gas may be able to stop the division of a certain type of somatic cells, meaning it could be possible to inhibit the proliferation of cancer cells. After that, nitrogen mustard gas (bis(2-chloroethyl)methylamine) (Figure 1, B) was developed and tested first on animals, and then on people. The results showed that these chemicals stopped the division of cancer cells (1).

According to this investigation, this new chemical was the milestone of cancer treatment. Since then, scientists have focused on developing new molecules to cure cancer.

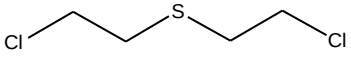

A: Bis(2-chloroethyl)sulfide

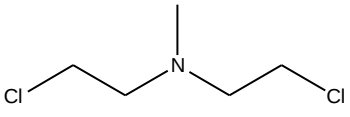

B: Bis(2-chloroethyl)methylamine

Figure 1. Mustard gases

Thiazolidine derivatives are molecules which exhibit cytotoxic activity against cancer cell lines. (*2RS,4R*)-2-phenyl-3-propinoyl-thiazolidine-4-carboxylic acid ethyl ester (ALC67) (Figure 2) is a thiazolidine-based antiproliferative molecule.

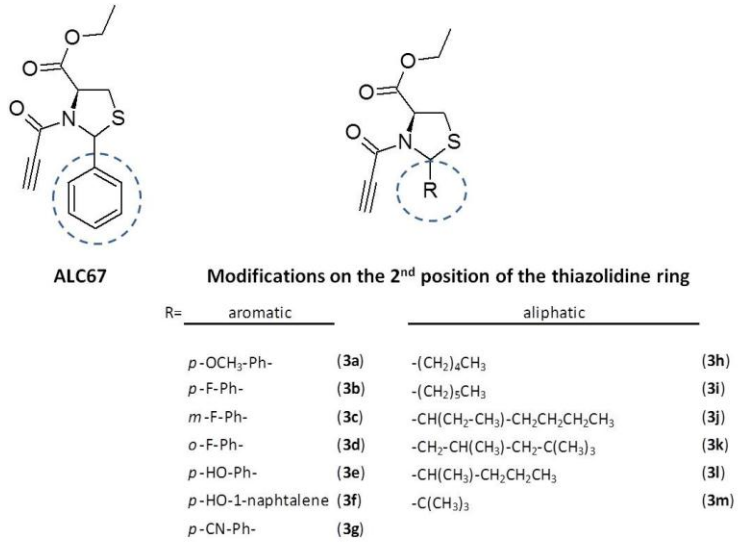

Figure 2. Structure of the ALC67 molecule and its derivatives.

Considering its bioactivity, this study aims to investigate the anticancer property of ALC67 derivatives. Actually, we will examine if any correlation exists between the presence of the phenyl group on the ALC67's structure and its cytotoxicity. For this purpose, the phenyl group will replaced with aromatic and aliphatic moieties.

2 GENERAL INFORMATION

2.1 Development of cancer

Cancer, a broad group of diverse diseases that can affect various organs, causes the death of 100 to 300 of each 100 000 people every year worldwide (1). It results from an abnormal proliferation of genetically altered cells (mutations or DNA damage) and this alteration often results from an excessive exposure to radiation, chemicals or some viruses (2).

Cancerization of normal cells requires defects on processes that control cell proliferation and homeostasis. There are six essential alterations that lead to tumorigenesis. These are sustaining proliferative signaling, evading growth suppressors, enabling replicative immortality, resisting programmed cell death (apoptosis), inducing angiogenesis and tissue invasion (Figure 3) (3, 4).

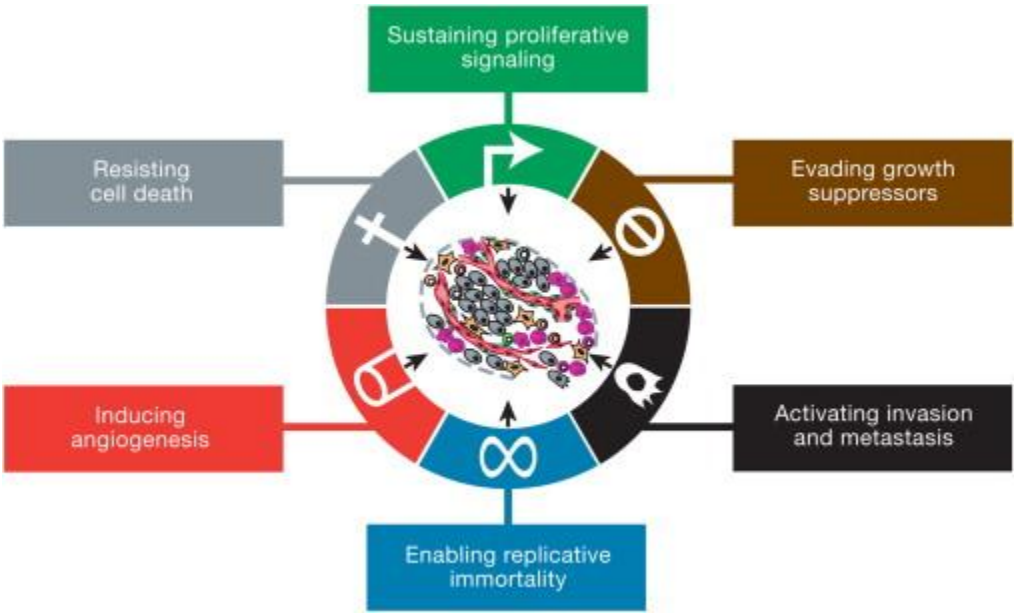

Figure 3. Hallmarks of cancer

Sustaining proliferative signals is one of the most important hallmarks of cancer cells. Normal cells need mitogenic growth factors (GF) to initiate proliferation. These factors are typically synthesized by cell types that are not related to the one that GFs stimulate. Therefore, proliferation is exogenously controlled in normal cells. Cancer cells, yet, were shown to acquire the capacity of synthesizing their own growth factors (as do, for instance, gliobastomas or

sarcomas by producing PDGF or TGFα) (5) an ability that makes them proliferate self-sufficiently.

In addition to the growth signal autonomy described above, cancer cells gain also an insensibility to antiproliferative signals when developing. In fact, while antigrowth signals prevent normal cells from excessive proliferation, they are ineffective in cancer cells since pathways that normally maintain cells in quiescence are disrupted in tumors (6).

The development of macroscopic malignant tumors also results from a limitless replicative potential of cancer cells. During cell division, telomeres, chromosome endings, are progressively shortened and after a critical length, cells stop growing or in other terms enter senescence. Thus the lifespan of normal cells is controlled by the length of telomeres. In cancer cells, it has been demonstrated that telomere lengths are maintained which provides them the ability of multiplying unlimitedly (7, 8).

Tumor cells can also expand rapidly *via* their ability of evasion from the programmed cell death process (PCD or apoptosis). Apoptosis is a natural death process that exists in almost all cell types. Once initiated, it triggers several physical changes such as cell shrinkage, membrane degradation or nuclear fragmentation. These changes lead then to the formation of apoptotic bodies that are subsequently phagocytized by adjacent macrophages (Figure 4) (9, 10).

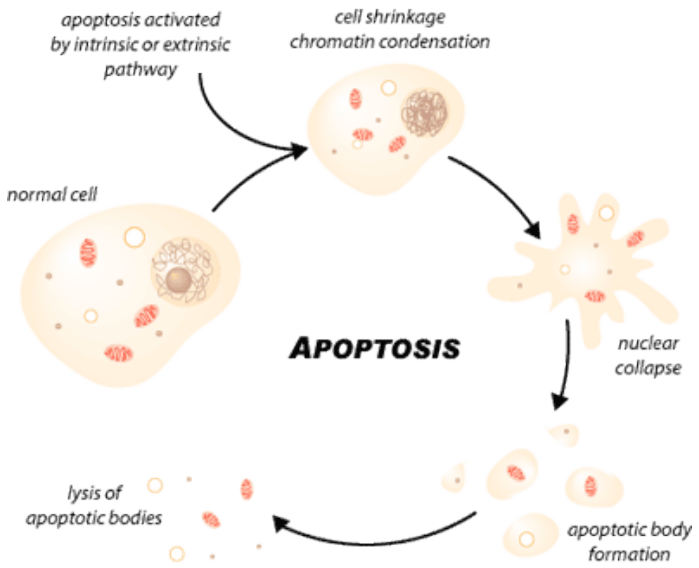

Figure 4. Apoptosis: the programmed cell death process.

Apoptosis starts with either extracellular or intracellular signals: it is activated exogenously when death signals such as FAS ligand or TNFα bind their corresponding receptors (11, 12), whereas intracellular death activator signals can be DNA damage (13), oncogene activation (14) or hypoxia (15, 16). The presence of these proapototic signals mainly switch on a class of cysteine-dependent aspartate specific proteases known as initator caspases. Initiator caspases activate then effector caspases that degrade cellular proteins to progressively destruct cellular structures, organelles and DNA (Figure 5) (17, 18). Tumor cells are shown to have multiple strategies to resist to apoptosis. For instance, the loss of function of the p53 tumor suppressor protein (19) an essential sensor that normally activates apoptosis, is the antiapoptotic feature that is the most observed in cancer cells (20-24).

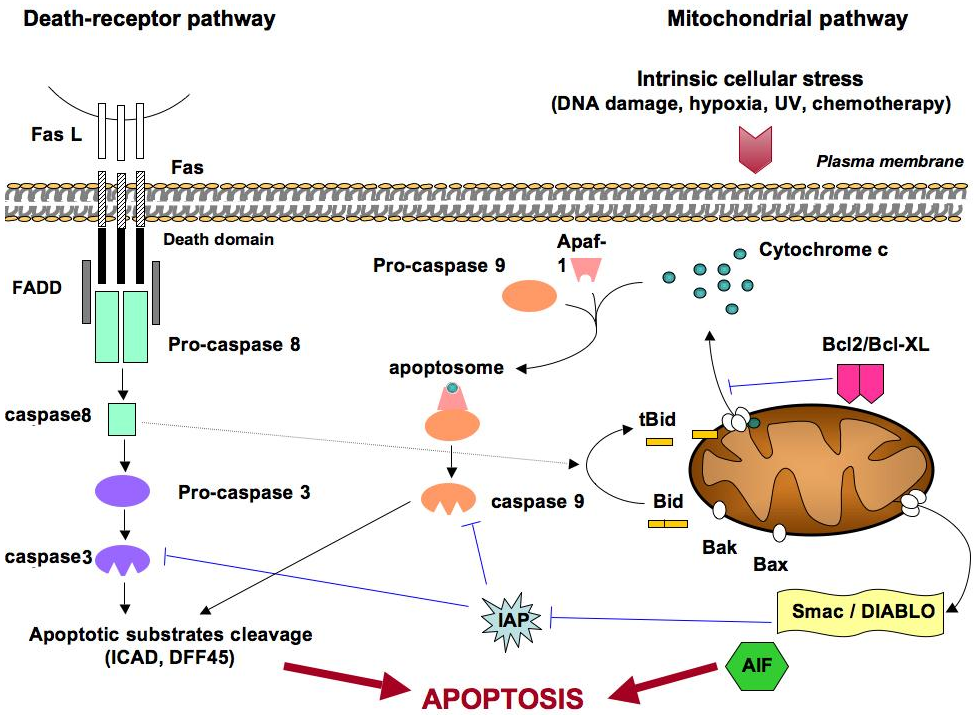

Figure 5. Extrinsic and intrinsic apoptotic pathways.

Factors mentioned above are related to tumor initiating and development processes. There are also two additional important capabilities that tumor cells acquire while developing: the ability to form new blood vessels in order to meet their needs in oxygen and nutrients (angiogenesis) and to invade adjacent (invasion) and distant tissues (metastasis). While sustained angiogenesis is related to a change in the balance of angiogenesis inducers and inhibitors (25-27) (overexpression of vascular endothelial growth factor VEGF (28) and fibroblast growth factor FGF (29, 30) and downregulation of inhibitors such as thrombospodin-1 or β-interferon) (31), metastasis that is the cause of 90% of human cancer death is ascribed to alterations in proteins involved in cell-cell or cell-extra cellular matrix adhesion (E-cadherin (32) and integrins respectively (33)).

Cancer treatment strategies aim to repair one of these abnormal abilities acquired by tumor cells. The most widely used chemotherapeutic agents either reinduce apoptosis in cancer cells, as it is the case for alkylating agents (cisplatins, tetrazins) (34), antimetabolites (anti-folates like methotrexate) (35), and topoisomerase inhibitors (doxorubicin, mitoxanthrone) (36) or prevent the neovascularization of tumors (paclitaxel, docetaxel) (37).

This study deals with the development of novel thiazolidine compounds that are able to act as apoptosis-inducers in cancer cells. Thus, the next section will be dedicated to the use of the thiazolidine ring in the literature for the development of proapoptotic anticancer agents.

2.2 Thiazolidines: Synthesis and NMR characterization

2.2.1 Synthesis

Thiazolidines are five-membered heterocycles containing a sulfur and a nitrogen atom at their 1st and 3rd positions respectively. They can be easily prepared from the acetalation of aldehydes with cysteine derivatives. The ring-closure reaction generates a chiral center, namely the carbon at the 2nd position. When reactions are conducted with optically pure cysteine derivatives, the resulting thiazolidine products come as diasteroemeric mixtures: using *L*-cysteine gives the 2R, 4R and 2S, 4R molecules whereas *D*-cysteine leads to the 2R, 4S and 2S, 4S compounds (Figure 6).

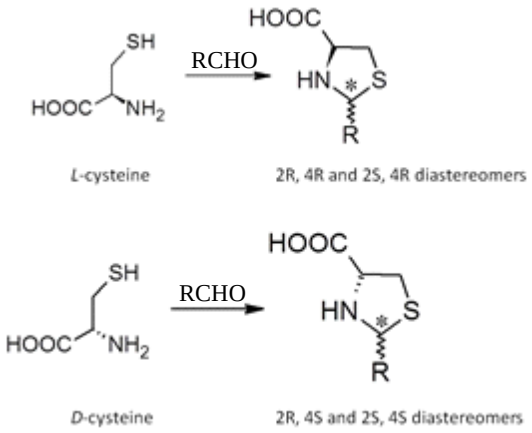

Figure 6. Leads thiazolidine formation to diastereomeric mixtures.

Thiazolidine formation can follow two possible mechanisms (38) that differ from each other by their first step: the first mechanism involves the formation of a cationic Shiff base with an addition-elimination sequence prior to the cyclisation (Figure 7, path 1) while the second begins with the attack of the sulfur atom on the carbonyl to form a sulfonium ion intermediate (Figure 7, path 2). Kinetic studies demonstrated that in alkali conditions the reaction follows path 1. It goes through a *N*-hydroxymethylcysteine that dehydrates to form the corresponding cationic Shiff base which rapidly deprotonates to give the expected heterocycle (38).

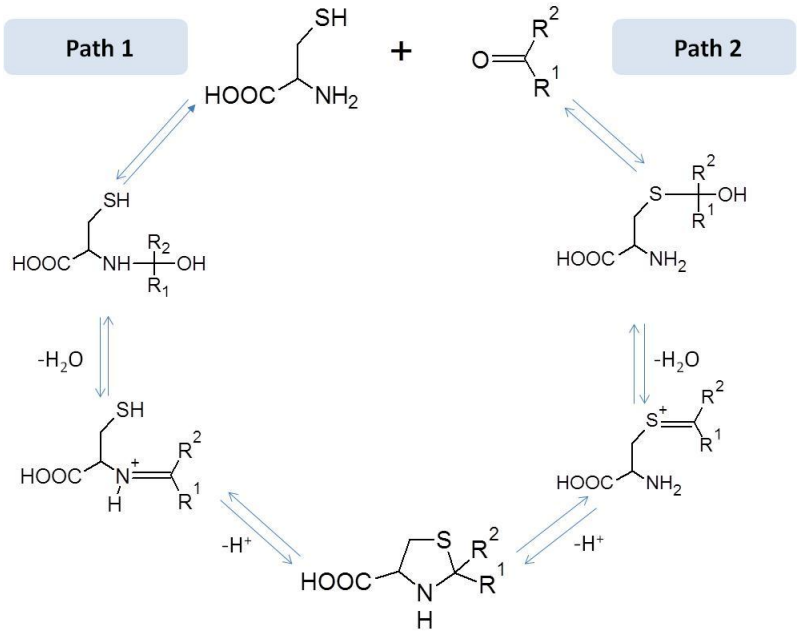

Figure 7. Possible pathways for the generation of a thiazolidine ring.

2.2.2 ^{1}H NMR characterization

The ^{1}H NMR spectrum of thiazolidine compounds obtained from the acetalation of pure cysteine present signals that correspond to the two diastereomers and the chemical shifts of the protons of each isomer are clearly separated and differ greatly. In fact, the cycle is characterized by the peaks corresponding to the C2-H, C4-H and C5-H, protons on the 5th carbon being unequivalent. C2-H signals appear as two separate singlets at around 5.50 and 5.35 ppm. The C4 protons that couple with both of the unequivalent C5 protons appear typically at around 4.20 and 3.80 ppm as doublet of doublets (dd) with coupling values of around 4.0 and 7.2 Hz for the minor isomer and 7.2 and 8.6 Hz for the major one, these values varying according to the group attached on C2. The C5 protons show four set of dds. Peaks for the minor isomer are centered at around 3.35 and 3.15 ppm with coupling values of around 4.0 (C4-H and C5-H coupling) and 10.0 Hz (C5-H and C5-H coupling) and 7.2 (C4-H and C5-H coupling) and 10.0 Hz (C5-H and C5-H coupling) respectively. Concerning the major isomer, C5-H dd signals appear around 3.30 and 3.05 ppm with J values of 7.2 (C4-H and C5-H coupling) and 10.0 Hz (C5-H and C5-H coupling) and 8.6 (C4-H and C5-H coupling) and 10.0 Hz (C5-H and C5-H coupling) (Figure 8).

The major diastereomer is expected to be the 2S, 4R molecule since in this configuration the two bulky groups, that are the R group that derives from the aldehyde and the carboxylic acid function, point to opposite sides of the thiazolidine ring. In fact, Yu *et al.* demonstrated this distribution by 1D nuclear Overhauser effect (NOE) experiments: while the irradiation of the signal of the C4-H of the major isomer (peak at around 4.20 ppm) did not generated any NOE signal with the corresponding C2-H peak (around 5.35 ppm), the C2-H (around 5.50 ppm) of the minor isomer gave a strong NOE signal when the corresponding C4-H (around 3.80 ppm) was irradiated. Results hence confirmed that the minor product is the 2R, 4R since it is with this configuration only that C2-H and C4-H protons are close enough to give NOE signals (39).

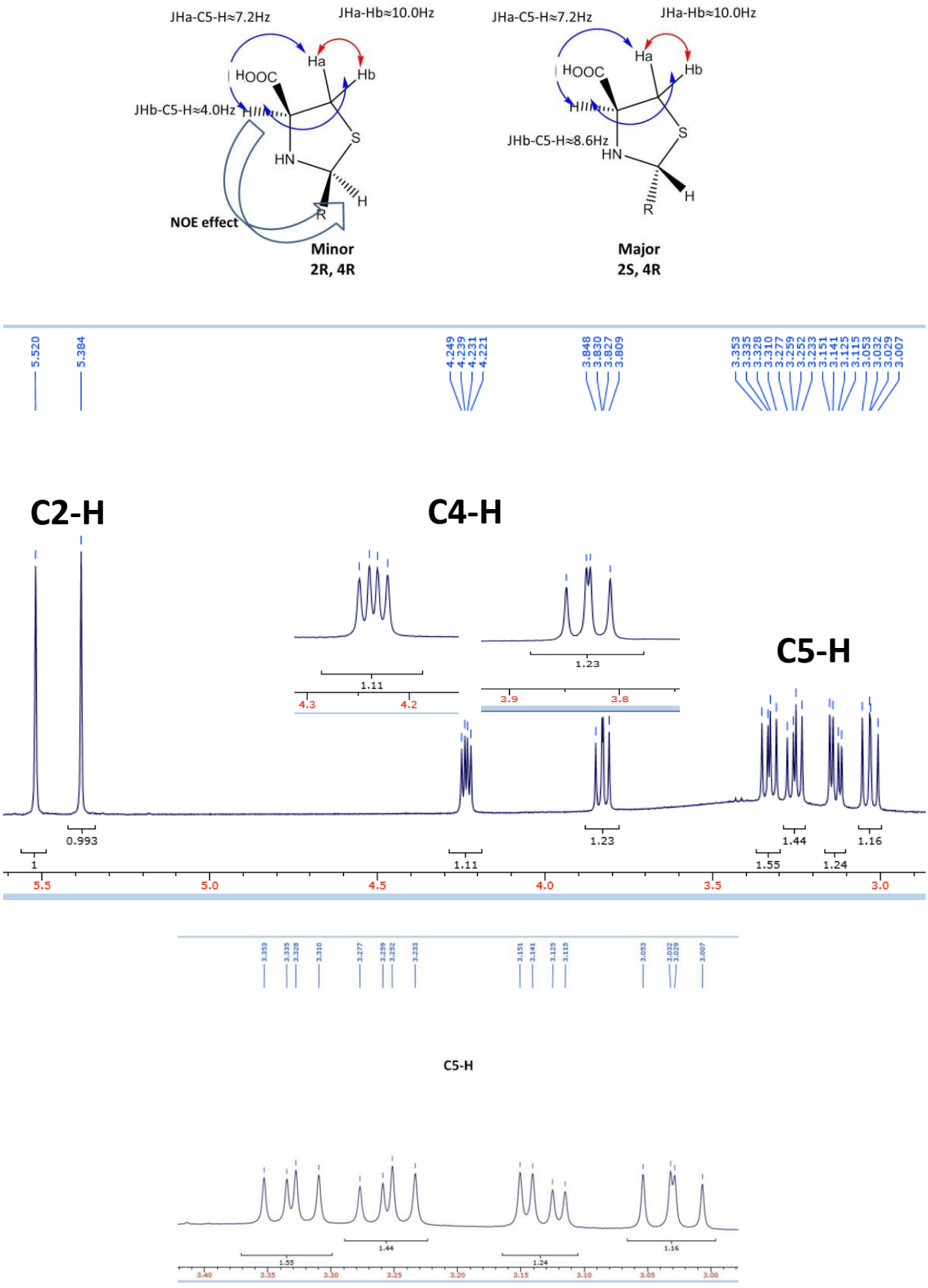

Figure 8. Typical [1]H NMR of thiazolidine rings obtained from acetalation of L-cysteine.

2.2.3 ^{13}C NMR characterization

The 2R, 4R and 2S, 4R thiazolidine heterocycles generated from the acetalation of *L*-cysteine can also be characterized by ^{13}C NMR. In this spectrum also, each carbon of each diastereomer gives separate signals, peaks appearing thus as pairs. The presence of the thiazolidine rings can be confirmed thanks to the presence of the signals correponding to the C2, C4 and C5 carbons. The tertiary C2 and C4 carbons appear upfield since they are close to the electronegative nitrogen atom. Indeed, while C2 typically gives two peaks around 71 ppm, for C4 two peaks appear around 65 ppm. Signals corresponding to the C5 of the isomers are located on downfield at around 38 ppm (Figure 9).

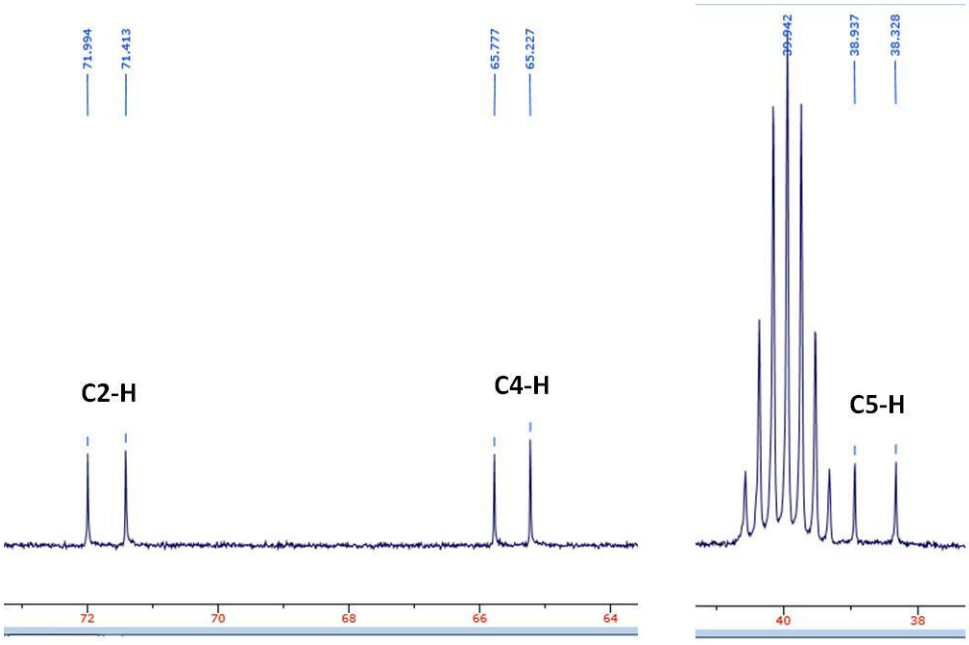

Figure 9. The characteristic ^{13}C NMR peaks of diastereomic mixture of thiazolidines.

2.3 Thiazolidines as anticancer agents

Thiazolidines were first described by Miller *et al.* for their anticancer property in 2005 (40). The authors developed thiazolidine compounds when optimizing the activity of 4-thiazolidinone derivatives.

2.3.1 Thiazolidines anticancer property derives from thiazolidinones' activity

4-Thiazolidinone presents a carbonyl group at the 4th position of the thiazolidine ring. This scaffold is actually well-known for its anti-inflammatory activity as thiazolidinone derivatives are described as effective cyclooxygenase (COX) inhibitors (41, 42). When high COX-2 expression levels were associated with certain cancer types, inhibitors of this enzyme were analyzed for their anticancer properties (43) and some 2-phenylimino-4-thiazolidinones were shown to exhibit promising cytotoxic activity (44). From that point, the potential of this scaffold for the development of novel anticancer agents was evaluated. Masoud *et al.* recently reported the antiproliferative activity of some benzimidazole substituted phenylimino-4-thiazolidinone derivatives (Figure 10) (44).

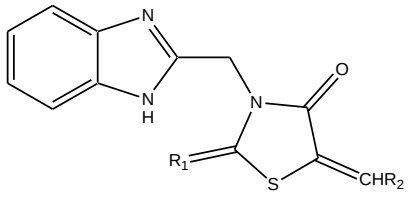

Figure 10. Benzimidazole substituted phenylimino-4-thiazolidinone derivatives

R_1: S, N-Ar; **R_2**: (*o*)ClC_6H_4, C_6H_5-CH=CH-, (*p*)$OCH_3C_6H_4$, 2,5-$(OCH_3)C_6H_3$, 2,4-$(OCH_3)C_6H_3$,C_5H_4N, C_6H_5, (*p*)$NO_2C_6H_4$.

Miller *et al.* discovered the antiproliferative activity of 4-thiazolidinone derivatives when they were optimizing some serine phosphate amides (SAPs) that they developed as lysophosphatidic acid (LPA) analogues to treat prostate cancer (Figure 11) (45).

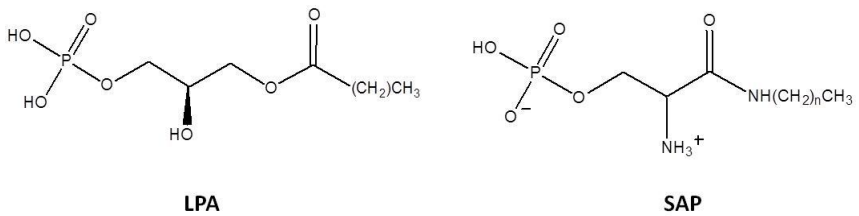

Figure 11. Structures of LPA and SAP.

Indeed, LPA is a molecule that induces prostate cell proliferation and was shown to exhibit mitogenic properties in prostate cancer cell lines (46, 47). By replacing the glycerol structure of LPA with a serine amide the authors developed a series of LPA antagonists (SAPs) with different alkyl chains (Scheme 1) that exhibited noteworthy cytotoxic activity on several prostate cancer cell lines (DU-145, PC-3, LNCaP, PPC-1 and TSU). However, these SAP molecules were shown to be non-selective since they also killed non-tumor chinese hamster ovary cells (45).

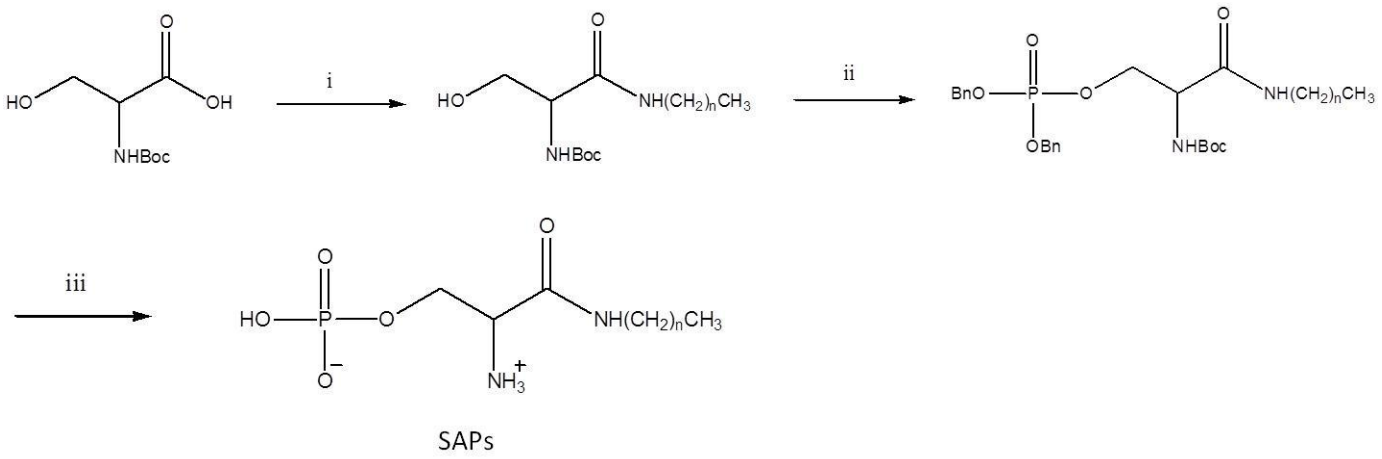

Scheme 1. Reagents and conditions for synthesis of SAPs derivatives

(i) $CH_3(CH_2)_nNH_2$, EDC, HOBt, CH_2Cl_2, RT, 5h. (ii) Tetrazole, Dibenzyldiisopropyl phosphoramidite, CH_2Cl_2, RT, 0.5h, H_2O_2, RT, 0.5h. (iii) H_2, 10% Pd/C, EtOH, RT, 3h.

To circumvent this selectivity issue that was attributed to the possible hydrolysis of the phosphate group present on the structures, the authors chose to work with 4-thiazolidinone derivatives as this cycle is described as a phosphate biomimetic (Figure 12) (48, 49).

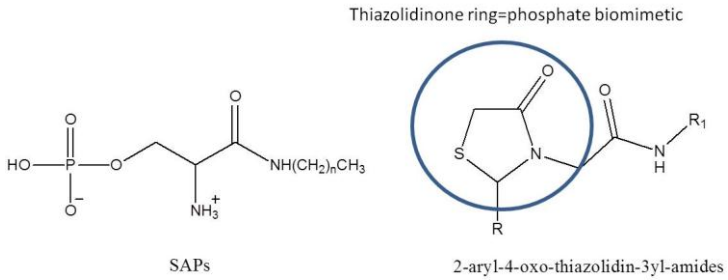

Figure 12. Structure of SAP and 4-thiazolidinone derivatives: 2-aryl-4-oxo-thiazolidin-3yl-amides.

The thiazolidinone heterocycles were generated through a condensation reaction between a mercapto acid, a glycine methyl ester and aromatic aldehydes. Then, thiazolidinone amides were obtained *via* peptidic couplings using EDC/HOBT as coupling agents (Scheme 2).

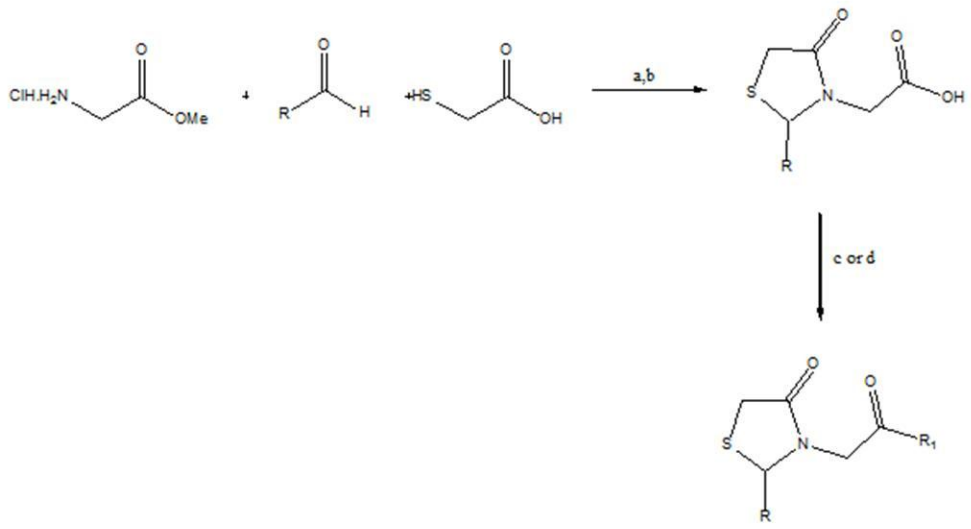

Scheme 2. Reagents and conditions for synthesis of thiazolidinone amides

Reagents: (a) toluene, Dean-Stark; (b) NaOH, MeOH; (c) $CH_3(CH_2)_nNH_2$, EDC, HOBt, CH_2Cl_2; (d) $(COCl)_2$, benzene, NH_3, MeOH.

Resulting derivatives were then evaluated on five human prostate cancer cell lines (DU-145, PC-3, LNCaP, PPC-1 and TSU) and despite an improved selectivity, these molecules exhibited disappointing cytotoxicity (48).

2.3.2 First antiproliferative thiazolidines: 2-arylthiazolidine-4-carboxylic acid amides (ATCAAs)

To improve the antiproliferative potency of 4-thiazolidinones, the thiazolidinone ring was replaced with a thiazolidine and a series of 2-arylthiazolidine-4-carboxylic acid amides (ATCAAs) was developed (40). Thiazolidines were obtained with the acetalation of optically pure cysteine and aldehydes (Scheme 3).

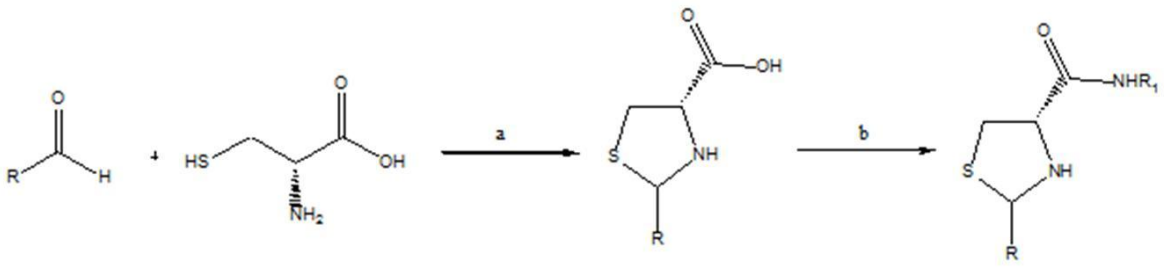

Scheme 3. Synthetis of ATCAAs

(a) EtOH; (b) $CH_3(CH_2)_nNH_2$, EDC, HOBt, CH_2Cl_2

Since the ring-closure reaction generates an additional chiral center in an uncontrolled manner, diastereomeric mixtures (2RS,4R) were obtained. Biological evaluations were carried out with these mixtures and promising cytotoxicities were observed on melanoma and prostate cancer cell lines. Then, to analyze the effect of the chiral center at the 4th position, the authors also prepared the (2RS,4S) thiazolidine compounds starting from *D*-cysteine but changing the chirality of the 4th position did not affect significantly neither the activity nor the selectivity. Besides, to investigate the impact of the thiazolidine ring on the biological activity, the authors examined the activity of analogue compounds exhibiting opened-thiazolidine rings (Figure 13) and observed a substantial decrease in the potency of the molecules. Thus, the bioactivity of ATCAAs was demonstrated to be closely related to the presence of the thiazolidine heterocyle.

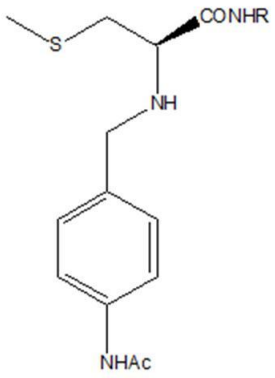

Figure 13. Structures of opened-ring compounds

The obtained ATCAA molecules were then evaluated against melanoma (A375, WM-164, B16-F1) and prostate (DU 145, PC-3, LNCaP, PCC-1) cancer cell lines and most of the analyzed

structures exhibited promising micromolar IC_{50} values (Table 1). Finally, to determine the origin of the biological activity, cell cycle analyses were also carried out on cancer cells exposed to different concentrations of ATCAAs and these molecules were shown to trigger cell death by apoptosis. Cytotoxic activity test of ATCAA compounds were performed on melanoma and prostate cancer cells in vitro. Acoording to the test results, compounds **3id**, **3ac** and **15b** had promising cytotoxic activity (40).

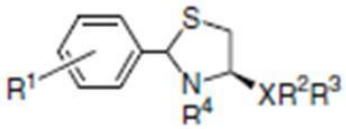

ID	X	R^1	R^2	R^3	R^4	IC_{50} ± SEM (μM)					
						B16-F1	A375	WM-164	Fibroblast	Aver.[a]	Ratio[b]
3aa	CON	3,4,5-Trimethoxy	n-$C_{18}H_{37}$	H	H	5.9 ± 0.4	4.6 ± 0.2	3.0 ± 0.1	4.7 ± 0.4	4.5	1.0
3ab	CON	3,4,5-Trimethoxy	(*Z*)-Octadec-8-enyl	H	H	4.7 ± 0.1	2.4 ± 0.1	1.3 ± 0.1	4.8 ± 0.3	2.8	1.7
3ac	CON	3,4,5-Trimethoxy	(*E*)-Octadec-8-enyl	H	H	3.2 ± 0.2	1.8 ± 0.1	1.1 ± 0.1	4.0 ± 0.3	2.0	2.0
3ad	CON	3,4,5-Trimethoxy	n-$C_{16}H_{33}$	H	H	1.6 ± 0.2	1.4 ± 0.2	0.7 ± 0.1	2.4 ± 0.4	1.2	2.0
3ba	CON	3,4-Dimethoxy	n-$C_{18}H_{37}$	H	H	14.3 ± 0.5	6.9 ± 0.3	2.7 ± 0.2	20.3 ± 1.1	8.0	2.5
3bb	CON	3,4-Dimethoxy	(*Z*)-Octadec-8-enyl	H	H	3.3 ± 0.2	1.6 ± 0.1	1.2 ± 0.1	18.3 ± 0.8	2.0	9.0
3bc	CON	3,4-Dimethoxy	(*E*)-Octadec-8-enyl	H	H	3.2 ± 0.3	1.4 ± 0.1	1.1 ± 0.1	16.3 ± 0.7	1.9	8.6
3ca	CON	2-OMe	n-$C_{16}H_{33}$	H	H	4.3 ± 0.2	3.0 ± 0.4	2.4 ± 0.2	7.2 ± 0.3	3.2	2.2
3da	CON	3-OMe	n-$C_{16}H_{33}$	H	H	3.0 ± 0.1	1.8 ± 0.1	1.2 ± 0.1	2.5 ± 0.2	2.0	1.3
3ea	CON	4-OMe	n-$C_{16}H_{33}$	H	H	2.3 ± 0.3	1.5 ± 0.1	1.0 ± 0.1	8.1 ± 0.5	1.6	5.1
3fa	CON	4-NMe_2	n-$C_{16}H_{33}$	H	H	6.7 ± 0.5	1.8 ± 0.1	1.5 ± 0.1	21.0 ± 3.1	3.3	6.3
3ga	CON	2-NHAc	n-$C_{16}H_{33}$	H	H	8.0 ± 0.4	9.3 ± 0.6	3.9 ± 0.5	27.8 ± 3.6	7.1	3.9
3ha	CON	3-NHAc	n-$C_{16}H_{33}$	H	H	2.2 ± 0.2	1.5 ± 0.1	1.1 ± 0.1	6.3 ± 0.4	1.6	3.9
3ia	CON	4-NHAc	n-$C_{18}H_{37}$	CH_3	H	18.9 ± 1.3	20.6 ± 2.1	10.7 ± 0.9	>100	16.7	–
3ib	CON	4-NHAc	1-Adamantanyl	H	H	96.5 ± 3.6	137.5 ± 4.2	127.5 ± 2.8	>100	120.5	–
3ic	CON	4-NHAc	2-Adamantanyl	H	H	108.2 ± 4.6	66.0 ± 2.4	64.4 ± 3.0	>100	79.5	–
3id	CON	4-NHAc	9*H*-Fluoren-2-yl	H	H	3.9 ± 0.3	2.1 ± 0.1	1.7 ± 0.1	28.9 ± 1.0	2.6	11.3
3ie	CON	4-NHAc	Anthracen-2-yl	H	H	5.6 ± 0.2	3.1 ± 0.1	1.4 ± 0.1	13.5 ± 0.5	3.4	4.0
3if	CON	4-NHAc	4-Biphenyl	H	H	5.7 ± 0.3	6.2 ± 0.4	4.1 ± 0.2	33.4 ± 3.5	5.3	6.3
3ig	CON	4-NHAc	2-Benzothiazolyl	H	H	55.3 ± 2.9	45.9 ± 3.7	>100	>100	50.6	-
3ih	CON	4-NHAc	(*Z*)-Hexadec-9-enyl	H	H	2.1 ± 0.1	1.9 ± 0.1	2.0 ± 0.1	14.0 ± 0.9	2.0	7.0
3ii	CON	4-NHAc	Nonadec-10-ynyl	H	H	1.6 ± 0.1	2.7 ± 0.2	1.3 ± 0.1	7.0 ± 0.3	1.9	3.8
3jb	CON	H	(*Z*)-Octadec-8-enyl	H	H	6.0 ± 0.5	4.9 ± 0.7	2.4 ± 0.1	11.6 ± 0.8	4.4	2.6
3jc	CON	H	(*E*)-Octadec-8-enyl	H	H	10.1 ± 0.8	5.3 ± 0.4	2.4 ± 0.2	12.4 ± 1.1	5.9	2.1
4	CON	4-NHAc	n-$C_{16}H_{33}$	H	Ac	15.0 ± 0.8	12.6 ± 0.5	20.4 ± 0.8	57.7 ± 1.3	16	3.6
5	COO	4-NHAc	n-$C_{16}H_{33}$	H	H	41.9 ± 3.1	28.0 ± 2.1	18.5 ± 0.4	>100	29.5	–
8a	CH_2N	H	n-$C_{16}H_{33}$	H	H	4.7 ± 0.2	13.0 ± 0.3	4.9 ± 0.1	60 ± 1.2	7.5	8.0
8b	CH_2N	4-NHAc	n-$C_{16}H_{33}$	H	H	11.9 ± 0.4	14.4 ± 0.3	3.2 ± 0.1	84.5 ± 2.5	9.8	8.6
15a	CON	4-$NHSO_2CH_3$	n-$C_{16}H_{33}$	H	H	113.6 ± 2.1	50.6 ± 1.6	18.6 ± 1.0	>100	60.9	-
15b	CON	4-$NHCOCH_2Cl$	n-$C_{16}H_{33}$	H	H	93.3 ± 3.6	20.4 ± 1.3	5.7 ± 0.2	25.4 ± 1.3	39.8	0.6
15c	CON	4-$NHCONH_2$	n-$C_{16}H_{33}$	H	H	6.5 ± 0.6	3.6 ± 0.3	1.7 ± 0.1	7.2 ± 0.4	3.9	1.8
1a	CON	H	n-$C_{18}H_{37}$	H	H	15.5 ± 0.6	15.0 ± 0.5	4.4 ± 0.2	29.8 ± 2.1	11.6	2.6
1b	CON	4-NHAc	n-$C_{16}H_{33}$	H	H	2.2 ± 0.3	2.1 ± 0.2	1.1 ± 0.1	16.0 ± 2.5	1.8	8.9
DTIC						>100	>100	>100	>100	–	–
CDDP						>100	>100	>100	>100	–	–
Sorafenib						4.9 ± 0.3	5.4 ± 0.5	5.0 ± 0.2	15.1 ± 1.2	5.1	3.0

Average IC_{50} of three melanoma cells IC_{50}s.

Table 1. IC_{50} values of ATCAA derivatives on melanoma and prostate cancer cell lines

2.3.3 ALC67: An apoptotic thiazolidine derivative

Based on findings that revealed the anticancer property of ATCAAs, Onen-Bayram *et al.* developed a library of small molecules around the thiazolidine scaffold that contained pyrimidine, benzoyl and triazole derivatives (Figure 14) (50). Molecules and their precursors were then screened on HUH7 hepatocellular carcinoma cells to analyze their cytotoxicity.

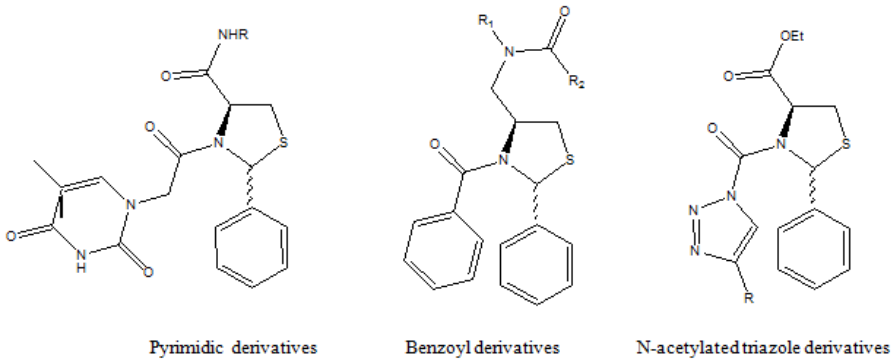

Figure 14. The small-molecule library around the thiazolidine scaffold

Interestingly although none of the final compounds showed any antiproliferative activity, the (*2RS,4R*)-2-phenyl-3-propionyl-thiazolidine-4-carboxylic acid ethyl ester (ALC67) a precursor of the triazole derivatives synthesized from the acylation of the secondary nitrogen of the thiazolidine ring with propiolic acid (Scheme 4), exhibited promising activity (IC_{50}= 5.30±0.93μM) (50).

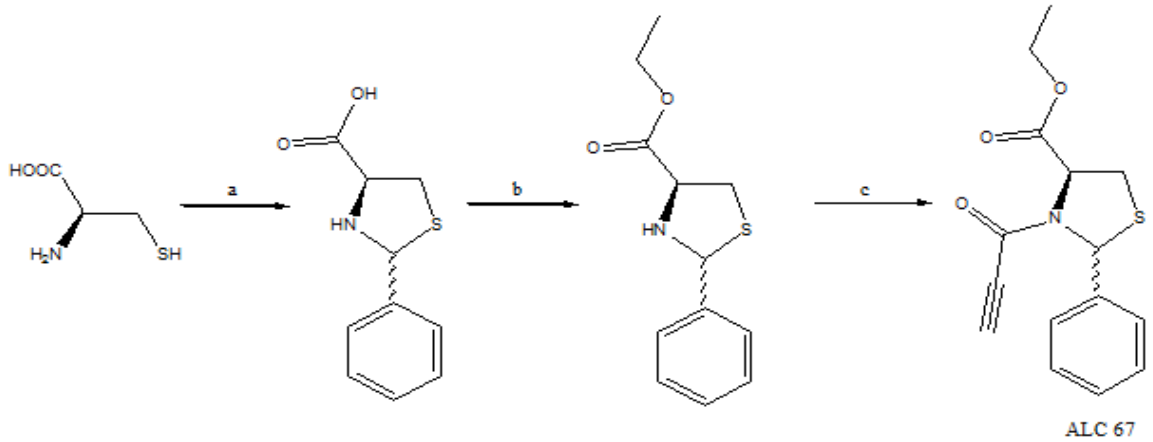

Scheme 4. Preparation of ALC 67

Reagents: (a) benzaldehyde in C_2H_5OH, H_2O (1:1); (b) $SOCl_2$ in absolute C_2H_5OH; (c) propiolic acid, DCC in dry DCM.

To analyze in depth the potency of this molecule, studies were carried out on some other liver cancer cells (HEPG2, Mahlavu, Focus) as well as breast (T47D, MCF7, BT20, CAMA-1), endometrial (MFE-296) and colon (HCT116) cancer cells and promising cytotoxicities of ALC67 were also obtained with these cell lines (Table 2). Furthermore, the authors established that the cell death was induced through apoptosis, ALC67 enhancing caspase-9 activity (50).

Tissue	Cell line	ALC 67 IC_{50} (µM)	CPT IC_{50} (µM)	5FU IC_{50} (µM)
Liver	HepG2	10.0 ± 1.5	0.0100	5.70
	Huh7	5.30 ± 0.93	0.150	30.7
	MV	0.41 ± 0.50	<1	9.97
	FOCUS	5.47 ± 1.50	<1	7.69
Colon	HCT116	9.23 ± 0.89	<1	18.7
Breast	T47D	7.62 ± 1.73	<1	8.91
	MCF7	4.70 ± 0.81	<1	3.50
	BT20	1.60± 0.56	0.00700	47.37
	CAMA-1	0.0100 ± 0.42	0.00700	1.28
Endometrial	MFE-296	0.50 ± 0.30	<1	30.7

Table 2. IC_{50} values of ALC 67 in liver, breast, colon, and endometrial cancer cell lines.

2.3.4 [Indoline-3,2'-thiazolidine]-based apoptotic compounds

To the best of our knowledge, there is no other study that deals with the efficient antiproliferative activity of simple thiazolidines. Very recently, Bertamino *et al*. published the proapoptotic activity of some [indoline-3,2'thiazolidine] compounds that present very rigid heterocyclic structures (51). These compounds were shown to mimic critical amino acid residues of the p53 protein. p53 is a tumor suppressor protein that regulates apoptosis. It has been shown that this protein loses its activity in cancer cells either by deletion, mutation or overexpression of the MDM2 protein that binds it and repress its action (21, 52). Thus a possible anticancer strategy would consist on disrupting the p53-MDM2 interactions as p53 and consequently apoptosis are then reactivated in cancer cells (Figure 15) (53, 54).

Authors developed a series of spiro(oxindole-3,3'-thiazolidine) derivatives to mimic the Phe19, Trp23 and Leu26 residues of p53 that are known to be essential for MDM2 binding (55).

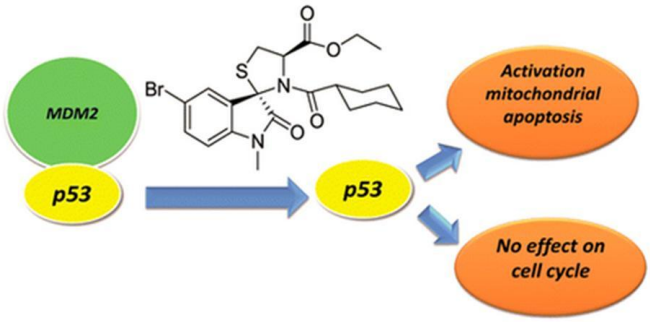

Figure 15. Inhibition of p53-MDM2 interaction with spiro(oxindole-3,3'-thiazolidine) derivatives

The analysis of the cyctotoxicity of obtained molecules on breast (MCF-7) and colon (HT29) cancer cell lines revealed the considerable potency of these structures as anticancer agents. Especially, **4n** showed high efficacy on breast (MCF-7) and colon (HT29) cancer cell lines (Table 3).

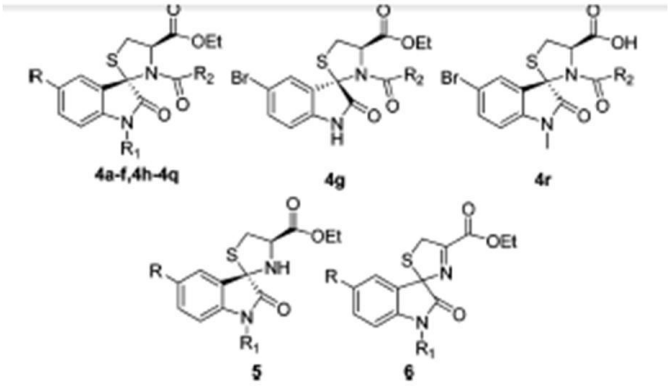

compd	R	R_1	R_2	$IC_{50} \pm SD$ (μM)[a] MCF-7[b]	HT29[c]
3	H	H		1.21 ± 0.6	1.60 ± 0.4
4a	H	H	$CH_2C_6H_4$(4-Cl)	>5	1.00 ± 0.2
4b	CH_3	H	$CH_2C_6H_4$(4-Cl)	4.81 ± 1.0	0.78 ± 0.2
4c	Br	H	$CH_2C_6H_4$(4-Cl)	2.90 ± 0.8	0.66 ± 0.1
4d	H	H	C_6H_4(4-Cl)	2.15 ± 0.7	3.69 ± 0.9
4e	CH_3	H	C_6H_4(4-Cl)	2.12 ± 0.7	1.09 ± 0.6
4f	Br	H	C_6H_4(4-Cl)	0.90 ± 0.2	0.11 ± 0.09
4g	Br	H	C_6H_4(4-Cl)	3.00 ± 0.2	2.00 ± 0.8
4h	H	CH_3	C_6H_4(4-Cl)	4.52 ± 1.1	0.18 ± 0.09
4i	CH_3	CH_3	C_6H_4(4-Cl)	1.23 ± 0.4	0.12 ± 0.07
4j	Br	CH_3	C_6H_4(4-Cl)	0.52 ± 0.3	0.08 ± 0.01
4k	Br	CH_3	$CH_2C_6H_4$(4-Cl)	0.27 ± 0.1	0.36 ± 0.09
4l	Br	CH_3	C_6H_5	0.31 ± 0.1	0.21 ± 0.2
4m	Br	CH_3	C_6H_4(4-CH_3)	0.06 ± 0.05	0.09 ± 0.05
4n	Br	CH_3	cyclohexyl	0.04 ± 0.01	0.07 ± 0.01
4o	CH_3	CH_3	cyclohexyl	1.20 ± 0.6	1.10 ± 0.6
4p	H	CH_3	cyclohexyl	2.30 ± 0.8	1.90 ± 0.8
4q	Br	H	cyclohexyl	0.22 ± 0.1	0.56 ± 0.1
4r	Br	CH_3	cyclohexyl	2.01 ± 0.9	1.90 ± 0.7
5a	H	COC_6H_4(4-Cl)	H	1.01 ± 0.6	1.03 ± 0.8
5b	CH_3	COC_6H_4(4-Cl)	H	3.46 ± 0.9	0.23 ± 0.1
5c	Br	COC_6H_4(4-Cl)	H	0.15 ± 0.1	0.02 ± 0.01
5d	Br	cyclohexyl	H	2.08 ± 0.8	1.40 ± 0.8
6b	CH_3	COC_6H_4(4-Cl)		2.78 ± 0.9	0.21 ± 0.1
6c	Br	COC_6H_4(4-Cl)		0.86 ± 0.4	0.20 ± 0.1
6d	Br	cyclohexyl		1.63 ± 0.6	0.85 ± 0.4

Table 3. IC_{50} values of indoline-thiazolidine derivatives on MCF7 and HT29 cancer cell lines.

Hence, they demonstrated the possible use of thiazolidine rings for the development of potent anticancer compounds (51).

2.4 ALC67 derivatives: Development of novel antiproliferative thiazolidine compounds

In this study we aimed to develop novel antiproliferative thiazolidine derivatives based on previous work that was carried out for the development of the ALC67 molecule. During the screening assays that revealed the cytotoxicity of this molecule, as already mentioned, in addition to some triazole, pyrimidine and benzoyl thiazolidine derivatives, precursor molecules that led to their synthesis were also evaluated. These included the (*2RS,4R*)-2-phenyl-thiazolidine-4-carboxylic acid and the corresponding ethyl ester which after acylation gave ALC67 (Figure 16).

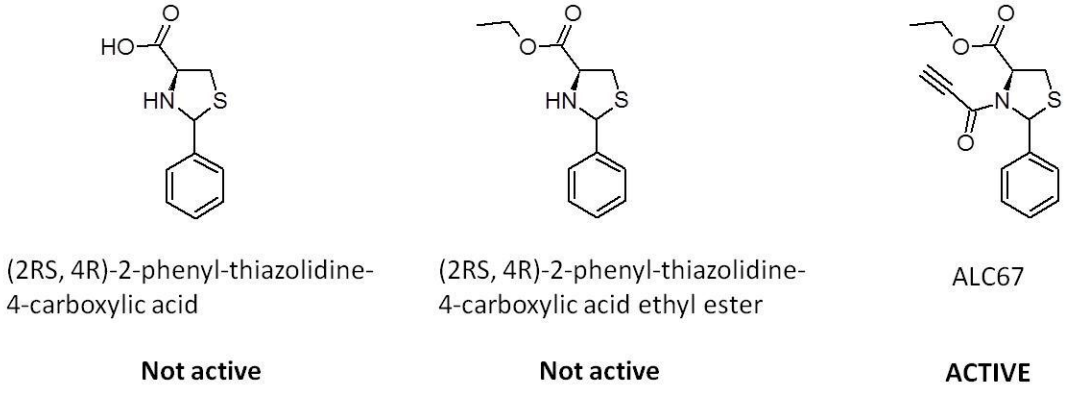

Figure 16. Two inactive molecules that are structurally related to ALC 67

These molecules did not show any activity. Since the structure of ALC67 differs only by the presence of the propionyl moiety on the heterocyclic nitrogen, we think that the cytotoxic property of this molecule is closely related to the presence of this moiety. That is why we decided to conserve the propargylic group when designed the novel thiazolidine derivatives to be prepared.

3 MATERIALS AND METHODS

3.1 Chemicals

All starting materials were commercially available used without further purification. *L*-cysteine hydrochloride monohydrate and hexanal were purchased from Merck KGaA. 4-methoxybenzaldehyde, 4-hydroxybenzaldehyde, 4-hydroxy-1-naphthalaldehyde, N-N'-Dicyclohexylcarbodiimide, pentanal, 2-methylpentanal, trimethylacetaldehyde and propiolic acid were purchased from Sigma–Aldrich. 4-Fluorobenzaldehyde, 3-fluorobenzaldehyde, 2-fluorobenzaldehyde and thionyl chloride were purchased from Fluka. 4-cyanobenzaldehyde were purchased from Alfa Aesar GmbH & Co. 2-ethylhexylaldehyde purchased from TCI America. 3,5,5-Trimethylhexanal purchased from SAFC.

3.2 Synthetic Procedures

3.2.1 General procedure for 1a-1m:

L-cysteine hydrochlorate monohydrate (1.0 eq) was dissolved in water, before adding sodium hydroxide (1.0 eq) and waiting for complete dissolution. Then, successivly, ethanol (EtOH), and aldehyde (1.0 eq) were added. The mixture was stirred at room temperature (RT) for three hours. Solid crystals that were formed, were filtered and washed with diethylether. The crystals were dried under *vacuo* to give the expected product.

3.2.2 General Procedure for 2a-2m:

Thionyl chloride (2.0 eq) was added in absolute EtOH at 0 ^{0}C. Then (*2RS,4R*) thiazolidine-4-carboxylic acid (1.0 eq) was added, the mixture was warmed to RT and stirred overnight. The mixture was concentrated at reduced pressure. Residue was dissolved in CH_2Cl_2 and washed with a saturated solution of $NaHCO_3$ (3x) and brine (1x). The organic layer was separated and dried over $MgSO_4$ and concentrated under reduced pressure.

3.2.3 General Procedure for 3a-3m:

Dicyclohexylcarbodiimide (DCC) (1.2 eq) was added to anhydrous CH_2Cl_2 at 0 ^{0}C, and propiolic acid (1.0 eq) was added drop by drop and stirred for ten minutes. Then (*2RS,4R*) thiazolidine-4-carboxylic acid ethyl ester (1.0 eq) was slowly added, and mixture was stirred at 0 ^{0}C for one

hour, before being stirred at room temperature overnight under inert atmosphere. Dicyclohexylcarbodiimide was removed by precipitation in diethylether and the extract was evaporated under reduced pressure. The resulting filtrate was purified flash chromatography. (ethylacetate:hexane 30:70)

3.3 Analytical Methods

3.3.1 Controls by Thin Layer Chromatography (TLC) solvent systems

Plates: In this work, Kieselgel 60 F_{254} (Merck) silica gel plaques were used for thin layer chromatography.

Solvent Systems: Solvent systems used in this work for the chromatographic controls of the compounds are given below.

ethyl acetate : *n*-hexane (30 : 70), ethyl acetate : *n*-hexane (50 : 50), ethyl acetate : methanol (90 : 10)

Elution Conditions: Solvent systems were poured to chambers and waited for saturation. Synthesized compounds and their starting materials dissolved in suitable solvents were applied to thin layer chromatography (TLC) plates and waited to drag at room temperature.

Identification of TLC spots: UV light (254 nm) was used for the detection of the spots.

Dyes:

Ninhydrin (Riedel-de Haen): A solution of 0.2 g ninhydrin in 100 mL ethanol.

Iodine vapor: Some crystals of iodine.

Phoshomolydbic acid: A solution of 0.25g molybdatophosphoric acid in 50 mL ethanol was used to dye spots on the TLC plate.

3.3.2 Spectrometric Analyses

3.3.2.1 Infrared Spectra:

Infrared (IR) spectra (10T/cm^2 pressure applied potassium bromide discs) were recorded on a Perkin Elmer FT-IR 1720X spectrometer and the frequencies were expressed in cm^{-1}.

3.3.2.2 ^{1}H-NMR Spectra:

The NMR spectra were recorded with a Bruker AC 400 Hz spectrometer, using tetramethylsilane as the internal reference, with chloroform ($CDCl_3$) and dimethylsulfoxide-d_6 as a solvent and chemical shifts were reported in parts per million (ppm).

3.3.2.3 ^{13}C-NMR Spectra:

The ^{13}C-NMR spectra of some compounds were recorded with a Bruker AC 400 Hz spectrometer.

3.3.2.4 LC-MS Spectra:

Spectra were recorded with a Waters 2695 Alliance Micromass ZQ LC-MS.

3.4 Activity Test Procedure: Sulforhodamine B Assay

Cells were plated in 96-well plates (1000-5000 cell/well in 200 µL) and grown for 24 h at 37 ^{0}C before being treated with various concentrations of the tested compounds (from 0.1 to 10 µM). After 72 hours of incubation the medium was aspirated, washed once with PBS ($CaCl_2$-, $MgCl_2$-free) (Gibco, Invitrogen), and then 50 µL of a cold (4 ^{0}C) solution of 10% (v/v) trichloroacetic acid (MERCK) was added. Microplates were left for 1 hour at 4 ^{0}C. After aspiration of the solution, plates were washed five times with deionized water and left to dry. Fifty microliter of a 0.4% (w/v) of sulforhodamine B (SRB) solution was removed and the plates washed five times with 1% acetic acid before air-drying. Bound sulforhodamine B solubilize in a 200 µL 10 mM Tris-base solution and the plates were left on a plate shaker for 10 min. The absorbance was read in a 96-well plate reader at 515 nm.

4 EXPERIMENTAL

4.1 Spectral data for 1a - 1m:

(2*RS*, 4*R*)-2-(4-Methoxyphenyl)-thiazolidine-4-carboxylic acid (1a)

$C_{11}H_{10}N_2O_2S$

M_W = 239.29 g.mol^{-1}

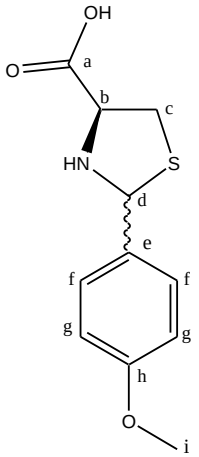

Yield: 66% (White crystal, 217 mg)

^{1}H NMR (DMSO-d_6) δ: 3.07 (t, *J*=9.6 Hz, 0.5H, H_c); 3.15 (dd, J_1=4.0 Hz, J_2=10.0 Hz, 0.5H, H_c); 3.29 (dd, J_1=7.2 Hz, J_2=10.4 Hz, 0.5H, H_c); 3.35 (dd, J_1=7.2 Hz, J_2=10.0 Hz, 0.5H, H_c); 3,74 (s, 1.5H, H_i); 3.76 (s, 1.5H, H_i); 3.87 (dd, J_1=7.2 Hz, J_2=8.4 Hz, 0.5H, H_b), 4.25 (dd, J_1=4.0 Hz, J_2=7.2 Hz, 0.5H, H_b); 5.46 (s, 0.5H, H_d); 5.60 (s, 0.5H, H_d); 6.89 (d, *J*=8.4 Hz, 1H, H_g); 6.92 (d, *J*=8.4 Hz, 1H, H_g); 7.37 (d, *J*=8.4 Hz, 1H, H_f); 7.44 (d, *J*=8.4 Hz, 1H, H_f).

^{13}C NMR (DMSO-d_6) δ: 37.8, 38.4 (C_c); 54.9, 55.0 (C_i); 64.7, 65.2 (C_b); 70.9, 71.4 (C_d); 113.5, 113.7 (C_g); 128.2, 128.4 (C_f); 130.6, 132.6 (C_e), 158.7, 159.1 (C_h); 172.2, 173.0 (C_a).

FT-IR (KBr), cm^{-1}: 3451 (O-H, carboxylic acid), 1583(C=O), 1480 (C=C, aromatic).

LC – MS: ELSD, rt = 3.40 min., *m/z* 240 $[M + H]^+$, 281 $[M + CH_3CN]^+$.

(2*RS*, 4*R*)-2-(4-Fluorophenyl)-thiazolidine-4-carboxylic acid (1b)

$C_{10}H_{10}FNO_2S$

$M_W = 227.26$ g.mol^{-1}

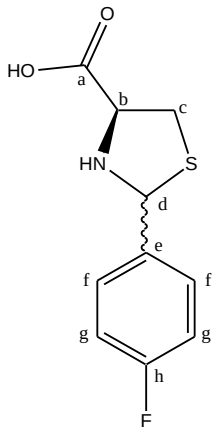

Yield: 65% (White crystal, 250 mg)

^{1}H NMR (DMSO-d_6) δ: 3.07 (dd, J_1= 8.8 Hz, J_2= 10.0 Hz, 0.8H, H_c); 3.12 (dd, J_1= 4.8 Hz, J_2= 10.0 Hz, 1.2H, H_c); 3.87 (dd, J_1= 7.2 Hz, J_2= 8.0 Hz, 0.4H, H_b); 4.19 (dd, J_1= 4.8 Hz, J_2= 8.0 Hz, 0.5H, H_b), 5.50 (s, 0.4H, H_d); 5.65 (s, 0.6H, H_d); 7.11-7.58 (m, 4H, $H_f + H_g$).

FT-IR (KBr), cm^{-1}: 2978 (O-H, carboxylic acid), 1483 (C=O), 1455 (C=C, aromatic).

LC – MS: ELSD, rt = 3.57 min., *m*/*z* 228 $[M + H]^+$, 269 $[M + CH_3CN]^+$.

(*2RS, 4R*)-2-(3-Fluorophenyl)-thiazolidine-4-carboxylic acid (1c)

$C_{10}H_{10}FNO_2S$

M_W = 227.26 g.mol^{-1}

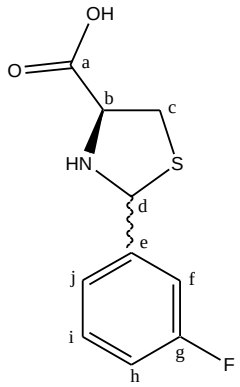

Yield: 74% (White crystal, 223 mg)

^{1}H NMR (DMSO-d_6) δ: 3.02 (dd, J_1=5.6 Hz, J_2=10.0 Hz, 1H, H_c); 3.27 (dd, J_1=6.4 Hz, J_2=10.0 Hz, 1H, H_c); 4.17 (t, J=6.4 Hz, 1H, H_b); 5.89 (s, 1H, H_d); 7.12-7.54 (m, 4H, H_f + H_h + H_i + H_j).

^{13}C NMR (DMSO-d_6) δ: 38.2, 38.5 (C_c); 64.0, 64.1 (C_b); 65.3, 65.8 (C_d); 115.5, 155.7 (C_f); 124.8, 127.5, 129.7, 158.7, 161.2 (C_{arom}); 172.6, 173.1 (C_a).

FT-IR (KBr), cm^{-1}: 2978 (O-H, carboxylic acid), 1575 (C=O), 1455 (C=C, aromatic).

LC – MS: ELSD, rt = 4.88 min., *m/z* 228 $[M + H]^+$, 269 $[M + CH_3CN]^+$.

(2*RS*, *4R*)-2-(2-Fluorophenyl)-thiazolidine-4-carboxylic acid (1d)

$C_{10}H_{10}FNO_2S$

Mw = 227.26 g.mol^{-1}

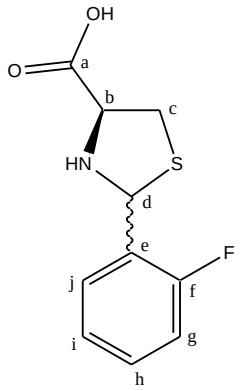

Yield: 73% (White crystal, 220 mg)

^{1}H NMR (DMSO-d_6) δ: 3.04 (m, 0.3H, H_c); 3.02-3.40 (m, 1.7H, H_c); 3.93 (q, J_1 = 6.8 Hz, J_2 = 9.2 Hz, 0.15H, H_b); 4.18 (t, J = 6.4 Hz, 0.85H, H_b); 5.69 (s, 0.15H, H_d); 5.91 (s, 0.85H, H_d); 7.14 - 7.42 (m, 3H, H_h + H_i + H_j); 7.55 (t, J = 7.2 Hz, 0.85H, H_g); 7.71 (t, J = 7.2 Hz, 0.15H, H_g).

FT-IR (KBr), cm^{-1}: 2978 (O-H, carboxylic acid), 1483 (C=O), 1455 (C=C, aromatic).

LC – MS: ELSD, rt = 2.93 min., *m*/*z* 228 $[M + H]^+$, 269 $[M + CH_3CN]^+$.

(2*RS*,4*R*)-2-(4-Hydroxyphenyl)-thiazolidine-4-carboxylic acid (1e)

$C_{10}H_{11}NO_3S$

Mw: 225.27 g.mol^{-1}

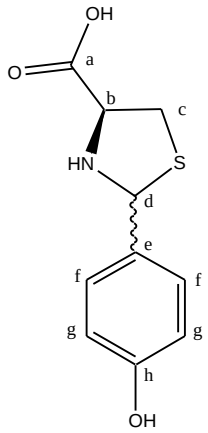

Yield: 70% (White crystal, 211 mg)

^{1}H NMR (DMSO-d_6) δ: 3.05 (dd, J_1=9.2 Hz, J_2=10.4 Hz, 0.5H, H_c); 3.15 (dd, J_1=3.6 Hz, J_2=10.0 Hz, 0.5H, H_c); 3.27 (dd, J_1=7.6 Hz, J_2=10.0 Hz, 0.5H, H_c); 3.35 (dd, J_1=7.2 Hz, J_2=10.0 Hz, 0.5H, H_c); 3.85 (dd, J_1=8.8 Hz, J_2=9.2 Hz, 0.5H, H_b), 4.25 (dd, J_1=4.0 Hz, J_2=7.2 Hz, 0.5H, H_b); 5.40 (s, 0.5H, H_d); 5.54 (s, 0.5H, H_d); 6.71 (d, J=8.8 Hz, 1H, H_g); 6.74 (d, J=8.8 Hz, 1H, H_g); 7.24 (d, J=8.4 Hz, 1H, H_f); 7.31 (d, J=8.8 Hz, 1H, H_f).

^{13}C NMR (DMSO-d_6) δ: 38.2, 38.9 (C_c); 65.1, 65.6 (C_b); 71.7, 72.3 (C_d); 115.4, 115.6 (C_f); 128.7, 129.0 (C_g); 129.3, 131.2 (C_e); 157.4, 157.8 (C_h); 172.7, 173.6 (C_a).

FT-IR (KBr), cm^{-1}: 3516 (O-H, phenol), 2984 (O-H, carboxylic acid), 1634 (C=O), 1615 (C=C, aromatic).

LC – MS: ELSD, rt = 4.56 min., *m*/*z* 226 $[M + H]^+$.

(2*RS*,4*R*)-2-(4-Cyanophenyl)-thiazolidine-4-carboxylic acid (1g)

$C_{11}H_{10}N_2O_2S$

M_W = 234.28 g.mol^{-1}

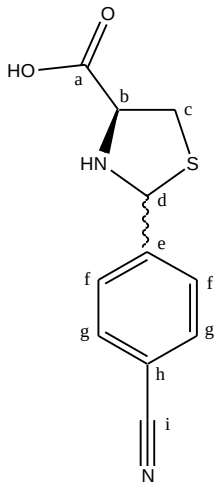

Yield: 63% (White crystal, 217 mg).

^{1}H NMR (DMSO-d_6) δ: 3.05-3.08 (m, 0.4H, H_c); 3.09 (t, *J*= 9.2 Hz, 0.6H, H_c); 3.32 (dd, J_1=6.8 Hz, J_2=10.0 Hz, 0.4H, H_c); 3.38 (dd, J_1=7.2 Hz, J_2=7.6 Hz, 0.6H, H_c); 3.94 (dd, J_1=7.2 Hz, J_2=8.8 Hz, 0.6H, H_b), 4.12 (t, *J*=6.4 Hz, 0.4H, H_b); 5.60 (s, 0.6H, H_d); 5.82 (s, 0.4H, H_d); 7.61 (d, *J*=8.0 Hz, 0.8H, H_f); 7.73 (d, *J*=8.0 Hz, 1.2H, H_f); 7.79 (d, *J*=8.4 Hz, 0.8H, H_g); 7.84 (d, *J*=8.0 Hz, 1.2H, H_g).

FT-IR (KBr), cm^{-1}: 3411 (N-H), 3002 (O-H, carboxylic acid), 2229 (C≡N), 1630 (C=O), 1505 (C=C, aromatic).

LC – MS: ELSD, rt = 3.44 min., *m*/*z* 235 $[M + H]^+$, 276 $[M + CH_3CN]^+$.

(*2RS, 4R*)-2-Pentyl-thiazolidine-4-carboxylic acid (1h)

$C_9H_{17}NO_2S$

Mw= 203.30 g.mol^{-1}

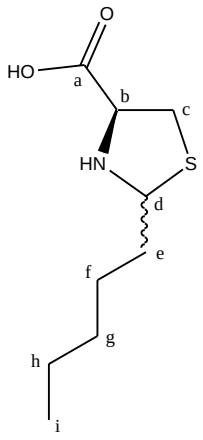

Yield: 90% (White crystal, 452 mg)

^{1}H NMR (DMSO-d_6) δ: 0.86 (t, *J*=6.8 Hz, 3H, H_i); 1.25-1.89 (m, 8H, H_h + H_g + H_f + H_e); 2.75 (t, *J*=9.6 Hz, 0.4H, H_c); 2.93 (dd, J_1=5.2 Hz, J_2=10.0 Hz, 0.6H, H_c); 3.08 (dd, J_1=6.8 Hz, J_2=10.0 Hz, 0.6H, H_c); 3.18 (dd, J_1=6.8 Hz, J_2=9.6 Hz, 0.4H, H_c); 3.69 (dd, J_1=6.8 Hz, J_2=9.6 Hz, 0.4H, H_b); 4.06 (dd, J_1=5.2 Hz, J_2=6.8 Hz, 0.6H, H_b); 4.40 (t, *J*=6.4 Hz, 0.4H, H_d); 4.54 (t, *J*=6.8 Hz, 0.6H, H_d).

FT-IR (KBr), cm^{-1}: 3435 (N-H), 2926 (O-H, carboxylic acid), 1614 (C=O).

LC – MS: ELSD, rt = 3.01 min., *m*/*z* 204 $[M + H]^+$, 245 $[M + CH_3CN]^+$.

(2*RS*, 4*R*)-2-Butyl-thiazolidine-4-carboxylic acid (1i)

$C_8H_{15}NO_2S$

Mw: 189.28 g.mol^{-1}

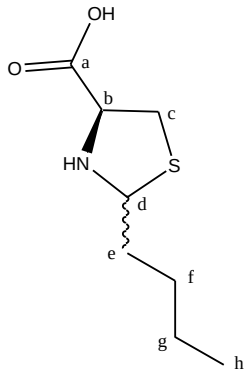

Yield: 36% (White crystal, 180 mg)

^{1}H NMR (DMSO-d_6) δ: 0.86 (t, *J*=7.0Hz, 1.5H, H_h); 0.87 (t, *J*=6.8 Hz, 1.5H, H_h); 1.26-1.94 (m, 6H, H_g + H_f + H_e); 2.75 (t, *J*=10.0 Hz, 0.5H, H_c); 2.93 (dd, J_1=5.2 Hz, J_2=10.0 Hz, 0.5H, H_c); 3.08 (dd, J_1=7.0 Hz, J_2=10.0 Hz, 0.5H, H_c); 3.18 (dd, J_1=7.0 Hz, J_2=10.0 Hz, 0.5H, H_c); 3.70 (dd, J_1=7.0 Hz, J_2=10.0 Hz, 0.5H, H_b); 4.06 (dd, J_1=5.2 Hz, J_2=7.0 Hz, 0.5H, H_b); 4.40 (t, *J*=6.4 Hz, 0.5H, H_d); 4.54 (t, *J*=6.8 Hz, 0.5H, H_d).

^{13}C NMR (DMSO-d_6) δ: 14.3, 14.3 (C_h); 22.3, 22.4 (C_g); 30.0, 30.2 (C_f); 35.0, 36.8 (C_e); 37.0, 37.4 (C_c); 64.6, 65.6 (C_b); 70.7, 71.5 (C_d); 172.7, 173.3 (C_a).

FT-IR (KBr), cm^{-1}: 2956 (O-H, carboxylic acid), 1580 (C=O).

LC – MS: ELSD, rt = 3.41 min., *m/z* 190 $[M + H]^+$, 231 $[M + CH_3CN]^+$.

(*2RS, 4R*)-2-(1-Ethylpentyl)-thiazolidine-4-carboxylic acid (1j)

$C_{11}H_{21}NO_2S$

Mw= 231.36 g.mol^{-1}

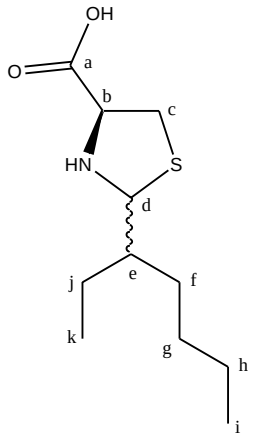

Yield: 92% (White crystal, 460 mg)

^{1}H NMR (DMSO-d_6) δ: 0.82-0.89 (m, 6H, H_i + H_k); 1.24-1.68 (m, 9H, H_e + H_f + H_g + H_h +H_j); 2.68 (t, *J*=9.6 Hz, 0.5H, H_c); 2.92 (dd, J_1=5.2 Hz, J_2=10.0 Hz, 0.5H, H_c); 3.01 (dd, J_1=6.8 Hz, J_2=10.0 Hz, 0.5H, H_c); 3.17 (dd, J_1=7.2 Hz, J_2=10.0 Hz, 0.5H, H_c); 3.70 (dd, J_1=7.2 Hz, J_2=9.6 Hz, 0.5H, H_b); 4.06 (dd, J_1=5.2 Hz, J_2=6.8 Hz, 0.5H, H_b); 4.41 (d, *J*=7.6 Hz, 0.5H, H_d); 4.52 (d, *J*=7.6 Hz, 0.5H, H_d).

FT-IR (KBr), cm^{-1}: 2963 (O-H, carboxylic acid), 1604 (C=O).

(2*RS*, 4*R*)-2-(2,4,4-trimethyl-pentyl)-thiazolidine-4-carboxylic acid (1k)

$C_{12}H_{23}NO_2S$

Mw: 245.38 g.mol^{-1}

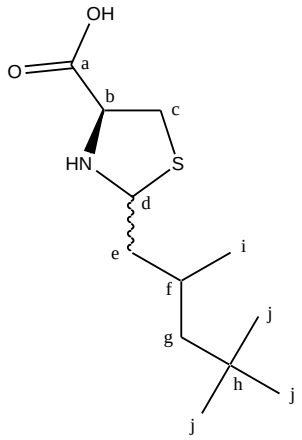

Yield: 80% (White crystal, 400 mg)

^{1}H NMR (DMSO-d_6) δ: 0.85-0.94 (m, 12H, H_i + H_j); 1.03-1.08 (m, 1H, H_g); 1.18-1.23 (m, 1H, H_g); 1.39-1.84 (m, 3H, H_e + H_f); 2.75 (td, J_1=4.0 Hz, J_2=10.0 Hz, 0.5H, H_c); 2.90-2.97 (m, 0.5H, H_c); 3.05-3.12 (m, 0.5H, H_c); 3.18 (dd, J_1=6.4 Hz, J_2=10.0 Hz, 0.5H, H_c); 3.70 (dd, J_1=7.2 Hz, J_2=10.0 Hz, 0.5H, H_b); 4.04-4.10 (m, 0.5H, H_b); 4.45 (t, J=6.4 Hz, 0.5H, H_d); 4.57-4.64 (m, 0.5H, H_d).

^{13}C NMR (DMSO-d_6) δ: 22.7, 22.75, 23.1, 23.2 (C_i); 28.1, 28.6, 28.6, 29.0 (C_f); 30.2, 30.3, 30.3, 30.4 (C_j); 31.2, 31.2, 31.3, 31.4 (C_h); 37.0, 37.3, 37.4, 37.6 (C_c); 44.9, 45.2, 46.4, 47.0 (C_e); 51.0, 51.6, 51.7 (C_g); 64.6, 64.63, 65.6, 65.7 (C_b); 68.9, 69.5, 69.6, 70.3 (C_d); 172.8, 173.3, 173.4 (C_a).

FT-IR (KBr), cm^{-1}: 2957 (O-H, carboxylic acid), 1611 (C=O).

LC – MS: ELSD, rt = 3.33 min., *m*/*z* 246 $[M + H]^+$, 287 $[M + CH_3CN]^+$.

(2*RS*, 4*R*)-2-(1-Methylbutyl)-thiazolidine-4-carboxylic acid (1l)

$C_9H_{17}NO_2S$

Mw= 203.10 g.mol^{-1}

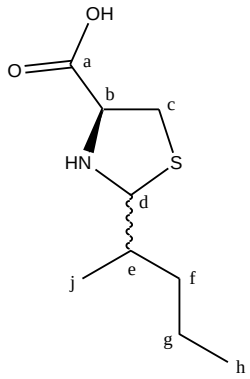

Yield: 61% (White crystal, 308 mg).

^{1}H NMR (DMSO-d_6) δ: 0.82-0.86 (m, 3H, H_h); 0.87 (d, *J*= 6.67 Hz, 0.75H, H_i); 0.91 (d, *J*= 6.67 Hz, 0.75H, H_i); 0.98 (d, *J*=6.67 Hz, 0.75H, H_i); 1.08-1.86 (m, 5H, H_g + H_f + H_e); 2.62-2.69 (m, 0.5H, H_c); 2.89 (dd, J_1= 5.0 Hz, J_2= 10.2 Hz, 0.5H, H_c); 3.00-3.03 (m, 0.5H, H_c); 3.12- 3.17 (m, 0.5H, H_c); 3.65-3.70 (m, 0.5H, H_b); 4.01-4.05 (m, 0.5H, H_b); 4.26 (d, *J*= 7.68 Hz, 0.25H, H_d); 4.31 (d, *J*= 7.13 Hz, 0.25H, H_d); 4.37 (d, *J*= 8.0 Hz, 0.25H, H_d); 4.41 (d, *J*= 7.50 Hz, 0.25H, H_d).

^{13}C NMR (DMSO-d_6) δ: 14.5, 14.6, 14.6, 14.7 (C_h); 17.0, 17.4, 17.6, 17.7 (C_j); 19.8, 19.9, 19.9, 20.0, (C_g); 36.8, 36.9, 36.9, 37.1 (C_f); 37.2, 37.2, 37.3, 37.3 (C_e); 37.4, 37.4, 37.5, 37.9 (C_c); 64.8, 64.9, 65.6 (C_b); 76.6, 76.7, 77.4, 77.5 (C_d); 172.8, 173.3, 173.4 (C_a).

FT-IR (KBr), cm^{-1}: 2960 (O-H, carboxylic acid), 1575 (C=O).

LC – MS: ELSD, rt = 4.95 min., *m*/*z* 204 $[M + H]^+$, 245 $[M + CH_3CN]^+$.

(2*RS*, 4*R*)-2-*tert*-Butyl-thiazolidine-4-carboxylic acid (1m)

$C_8H_{15}NO_2S$

Mw: 189.28 g.mol^{-1}

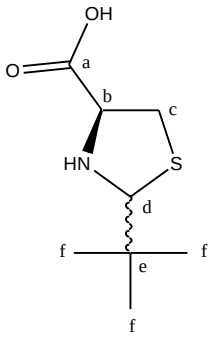

Yield: 59% (White crystal, 295 mg)

^{1}H NMR (DMSO-d_6) δ: 0.97 (s, 0.45H, H_f); 1.00 (s, 8.55H, H_f); 2.63 (t, *J*=10.0 Hz, 0.95H, H_c); 2.91-2.98 (m, 0.1H, H_c); 3.19 (dd, J_1=6.4 Hz, J_2=10.0 Hz, 0.95H, H_c); 3.70 (dd, J_1=6.4 Hz, J_2=10.0 Hz, 0.95H, H_b); 4.07-4.10 (m, 0.05H, H_b); 4.38 (s, 0.95H, H_d); 4.2 (s, 0.05H, H_d).

^{13}C NMR (DMSO-d_6) δ: 26.6, 26.7 (C_f); 33.5, 35.0 (C_e); 36.6, 38.7 (C_c); 64.91, 64.93 (C_b); 80.1, 81.2 (C_d); 172.3, 172.9 (C_a).

FT-IR (KBr), cm^{-1}: 3061 (O-H, carboxylic acid), 1642 (C=O).

LC – MS: ELSD, rt = 3.37 min., *m*/*z* 190 $[M + H]^+$, 231 $[M + CH_3CN]^+$.

4.2 Data for 2a – 2m

(2*RS*,4*R*)-2-(4-Methoxyphenyl)-thiazolidine-4-carboxylic acid ethyl ester (2a)

$C_{13}H_{17}NO_3S$

$M_W = 267.55$ g.mol^{-1}

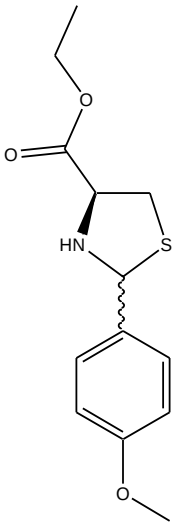

Yield: 35% (Yellow oil, 50 mg) Crude product was used without further purification for the next step.

(2*RS*,4*R*)-2-(4-Fluorophenyl)-thiazolidine-4-carboxylic acid ethyl ester (2b)

$C_{12}H_{14}FNO_2S$

Mw: 255.31 $g.mol^{-1}$

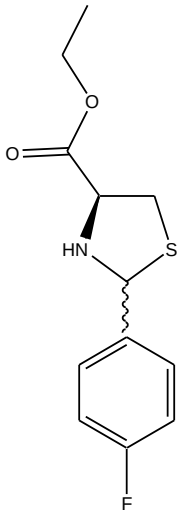

Yield: 50 % (Yellow oil, 85 mg) Crude product was used without further purification for the next step.

(2*RS*,4*R*)-2-(3-Fluorophenyl)-thiazolidine-4-carboxylic acid ethyl ester (2c)

$C_{12}H_{14}FNO_2S$

Mw: 255.31 $g.mol^{-1}$

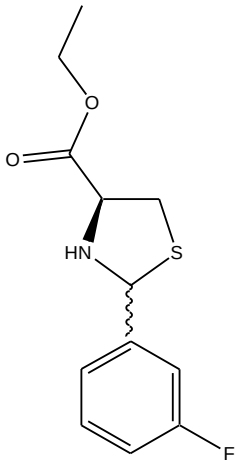

Yield: 66% (Yellow oil, 132 mg) Crude product was used without further purification for the next step.

(2*RS*, 4*R*)-2-(2-Fluorophenyl)-thiazolidine-4-carboxylic acid ethyl ester (2d)

$C_{12}H_{14}FNO_2S$

Mw = 255.31 $g.mol^{-1}$

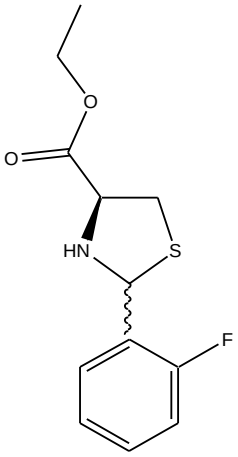

Yield: 33% (Yellow oil, 50 mg) Crude product was used without further purification for the next step.

(2*RS*,4*R*)-2-(4-Hydroxyphenyl)-thiazolidine-4-carboxylic acid ethyl ester (2e)

$C_{12}H_{15}NO_3S$

Mw: 253.32 $g.mol^{-1}$

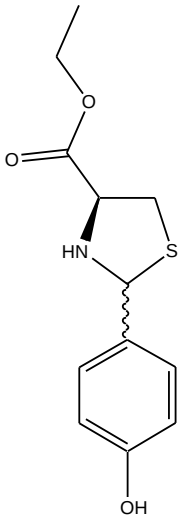

Yield: 38% (Yellow oil, 76 mg) Crude product was used without further purification for the next step.

(2*RS*,4*R*)-2-(4-Cyanophenyl)-thiazolidine-4-carboxylic acid ethyl ester (2g)

$C_{13}H_{14}NO_2S$

M_W = 248.32 $g.mol^{-1}$

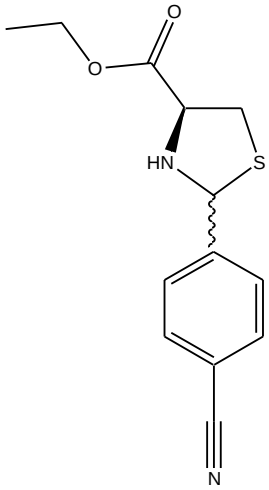

Yield: 46 % (Yellow oil, 150 mg) Crude product was used without further purification for the next step.

(2*RS*, 4*R*)-2-Pentyl-thiazolidine-4-carboxylic acid ethyl ester (2h)

$C_{11}H_{21}NO_2S$

Mw= 231.36 g.mol^{-1}

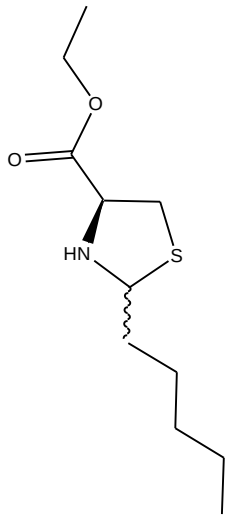

Yield: 62% (Yellow oil, 270 mg) Crude product was used without further purification for the next step.

(2*RS*, 4*R*)-2-Butyl-thiazolidine-4-carboxylic acid ethyl ester (2i)

$C_{10}H_{19}NO_2S$

Mw: 217.33 g.mol^{-1}

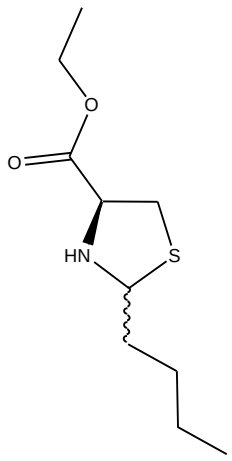

Yield: 90% (Yellow oil, 150 mg) Crude product was used without further purification for the next step.

(2*RS*, 4*R*)-2-(1-Ethylpentyl)-thiazolidine-4-carboxylic acid ethyl ester (2j)

$C_{13}H_{25}NO_2S$

Mw= 259.41 g.mol^{-1}

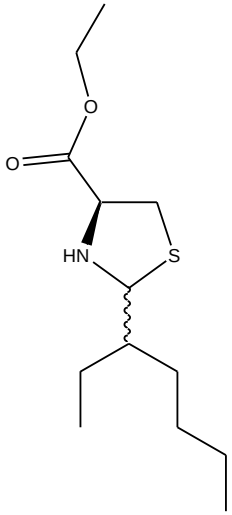

Yield: 61% (Yellow oil, 260 mg) Crude product was used without further purification for the next step.

(2*RS*, 4*R*)-2-(2,4,4-Trimethylpentyl)-thiazolidine-4-carboxylic acid ethyl ester (2k)

$C_{14}H_{27}NO_2S$

Mw: 273.44 g.mol^{-1}

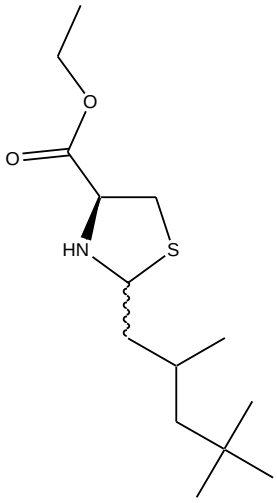

Yield: 76% (Yellow oil, 288 mg) Crude product was used without further purification for the next step.

(2*RS*, 4*R*)-2-(1-Methylbutyl)-thiazolidine-4-carboxylic acid ethyl ester (2l)

$C_{11}H_{21}NO_2S$

Mw= 231.36 g.mol^{-1}

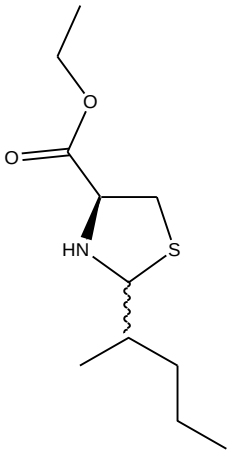

Yield: 93% (Yellow oil, 280 mg) Crude product was used without further purification for the next step.

(2*RS*,4*R*)-2-*tert*-Butyl-thiazolidine-4-carboxylic acid ethyl ester (2m)

$C_{10}H_{19}NO_2S$

Mw: 217.33 g.mol^{-1}

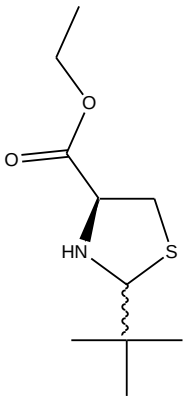

Yield: 77% (Yellow oil, 214 mg) Crude product was used without further purification for the next step.

4.3 Spectral data for 3a – 3m

(2*RS*,4*R*)-2-(4-Methoxyphenyl)-3-propynoyl-thiazolidine-4-carboxylic acid ethyl ester (3a)

$C_{16}H_{17}NO_4S$

M_W = 319.38 g.mol^{-1}

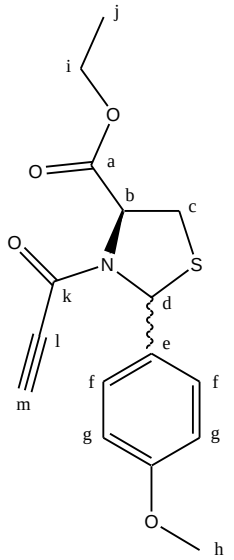

Yield: 89% (Yellow oil, 15 mg), R_f: 0.68 ethyl acetate:*n*-hexane (30:70)

^{1}H NMR ($CDCl_3$) δ: 1.29 (t, *J*= 7.2 Hz, 1.2H, H_j); 1.31 (t, *J*= 7.2 Hz, 1.8H, H_j); 2.96 (s, 0.6H, H_m); 3.08 (s, 0.4H, H_m); 3.27 (dd, J_1= 7.2 Hz, J_2= 12.4 Hz, 0.6H, H_c); 3.35 (dd, J_1= 6.8 Hz, J_2= 12.0 Hz, 0.6H, H_c); 3.41-3.43 (m, 0.8H, H_c); 3.79 (s, 1.2H, H_h); 3.81 (s, 1.8H, H_h); 4.21-4.33 (m, 2H, H_i); 4.98 (t, *J*= 7.2 Hz, 0.6H, H_b); 5.21 (t, *J*= 5.6 Hz, 0.4H, H_b); 6.33 (s, 0.4H, H_d); 6.41 (s, 0.6H, H_d); 6.85 (d, *J*= 8.8 Hz, 0.8H, H_g); 6.89 (d, *J*= 8.8 Hz, 1.2H, H_g); 7.51 (d, *J*= 8.8 Hz, 0.8H, H_f); 7.58 (d, *J*= 8.8 Hz, 1.2H, H_f).

FT-IR (KBr), cm^{-1}: 3441 (C-H, C≡C-H), 2108 (C≡C), 1741 (C=O, ester), 1635 (C=O, ketone), 1512 (C=C, aromatic).

(2*RS*,4*R*)-2-(4-Fluorophenyl)-3-propynoyl-thiazolidine-4-carboxylic acid ethyl ester (3b)

$C_{15}H_{14}FNO_3S$

Mw = 307.34 g.mol^{-1}

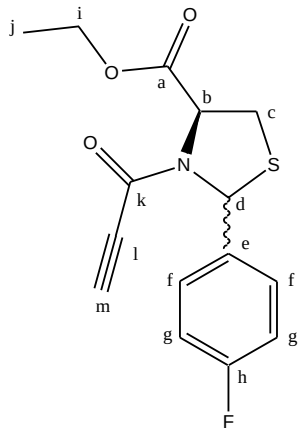

Yield: 37% (Yellow oil, 56 mg), R_f: 0.65 ethyl acetate:*n*-hexane (30:70)

^{1}H NMR ($CDCl_3$) δ: 1.25-1.36 (m, 3H, H_j); 2.96 (s, 0.6H, H_m); 3.10 (s, 0.4H, H_m); 3.25 (dd, J_1= 7.6 Hz, J_2= 12.0 Hz, 0.6H, H_c); 3.37 (dd, J_1= 6.8 Hz, J_2= 12.0 Hz, 0.6H, H_c); 3.44 (d, J=6.0 Hz, 0.8H, H_c); 4.22-4.32 (m, 2H, H_i); 4.99 (t, J= 7.2 Hz, 0.6H, H_b); 5.22 (t, J= 6.0 Hz, 0.4H, H_b); 6.33 (s, 0.5H, H_d); 6.42 (s, 0.5H, H_d); 7.00 (d, J= 8.4 Hz, 0.4H, H_g); 7.00 (d, J= 8.8 Hz, 0.4H, H_g); 7.05 (d, J= 8.8 Hz, 0.6H, H_g); 7.05 (d, J= 8.4 Hz, 0.6H, H_g); 7.57 (d, J= 8.4 Hz, 0.6H, H_f); 7.58 (d, J= 8.8 Hz, 0.4H, H_f); 7.64 (d, J= 8.4 Hz, 0.6H, H_f); 7.66 (d, J= 8.0 Hz, 0.4H, H_f).

^{13}C NMR (DMSO-d_6) δ: 14.0, 14.1 (C_j); 32.5, 33.5 (C_c); 62.3, 62.5 (C_i); 65.8, 65.3 (C_b); 63.7, 67.1 (C_d); 75.0, 75.3 (C_l); 81.2, 81.2 (C_m); 115.1, 115.2, 115.3, 115.4 (C_g); 128.6, 128.7, 129.0, 129.1 (C_f); 133.7, 135.5 (C_e); 152.3, 155.0 (C_h); 161.5, 163.5 (C_k); 168.9, 169.4 (C_a).

FT-IR (KBr), cm^{-1}: 3243 (C-H, C≡C-H), 2110 (C≡C), 1742 (C=O, ester), 1634 (C=O, ketone), 1510 (C=C, aromatic).

(2*RS*, 4*R*)-2-(3-Fluorophenyl)-3-propynoyl-thiazolidine-4-carboxylic acid ethyl ester (3c)

$C_{15}H_{14}FNO_3S$

Mw = 307.34 g.mol^{-1}

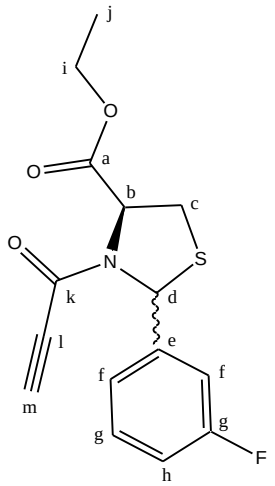

Yield: 58% (Yellow oil, 116 mg), R_f: 0.64 ethyl acetate:*n*-hexane (30:70)

^{1}H NMR ($CDCl_3$) δ: 1.35 (t, *J*=7.2 Hz, 2.1H, H_j); 1.37 (t, *J*=7.2 Hz, 0.9H, H_j); 2.93 (s, 0.3H, H_m); 2.98 (s, 0.7H, H_m); 3.28 (dd, J_1= 9.0 Hz, J_2= 12.0 Hz, 0.7H, H_c); 3.38 (dd, J_1= 6.6 Hz, J_2= 12.0 Hz, 0.7H, H_c); 3.40 (dd, J_1= 6.6 Hz, J_2 = 12.0 Hz, 0.3H, H_c); 3.46 (dd, J_1= 6.8 Hz, J_2= 12.0 Hz, 0.3H, H_c); 4.24 – 4.39 (m, 2H, H_i); 4.90 (dd, J_1= 6.4 Hz, J_2= 8.4 Hz, 0.3H, H_b); 5.18 (t, *J*= 6.4 Hz, 0.7H, H_b); 6.52 (s, 0.3H, H_d); 6.63 (s, 0.7H, H_d); 7.00 – 7.33 (m, 3H, H_f + H_h); 7.82 (td, J_1= 1.6 Hz, J_2= 8.0 Hz, 0.3H, H_g); 8.05 (td, J_1= 1.6 Hz, J_2= 8.0 Hz, 0.7H, H_g).

FT-IR (KBr), cm^{-1}: 3338 (C-H, C≡C-H), 2042 (C≡C), 1912 (C=O, ester), 1704 (C=O, ketone).

LC – MS: ELSD, rt = 5.48 min., *m*/*z* 308 $[M + H]^+$, 371 $[M + CH_3CN + Na]^+$.

(2*RS*,4*R*)-2-(2-Fluorophenyl)-3-propynoyl-thiazolidine-4-carboxylic acid ethyl ester (3d)

$C_{15}H_{14}FNO_3S$

Mw = 307.34 g.mol^{-1}

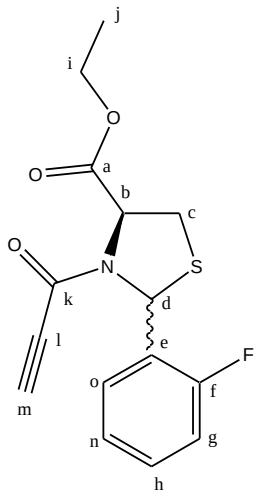

Yield: 30% (Yellow oil, 15 mg), R_f: 0.65 ethyl acetate:*n*-hexane (30:70)

^{1}H NMR ($CDCl_3$) δ: 1.34-1.38 (m, 3H, H_j); 2.93 (s, 0.7H, H_m); 2.98 (s, 0.3H, H_m); 3.29 (dd, J_1 = 8.0 Hz, J_2 =12.0 Hz, 0.7H, H_c); 3.37 (dd, J_1= 6.8 Hz, J_2=12.0 Hz, 0.7H, H_c); 3.39-3.48 (m, 0.6H, H_c); 4.12-4.40 (m, 2H, H_i); 4.90 (dd, J_1= 6.8 Hz, J_2= 9.2 Hz 0.7H, H_b); 5.18 (t, J= 6.4 Hz, 0.3H, H_b); 6.52 (s, 0.3H, H_d); 6.63 (s, 0.7H, H_d), 7.00-7.34 (m, 3H, H_o + H_n + H_g); 7.82 (td, J_1= 1.6 Hz, J_2= 8.0 Hz, 0.3H, H_h); 8.06 (td, J_1= 1.6 Hz, J_2= 8.0 Hz, 0.7H, H_h).

LC – MS: ELSD, rt = 5.45 min., *m*/*z* 308 $[M + H]^+$, 371 $[M + CH_3CN + Na]^+$.

(2*RS*,4*R*)-2-(4-Cyanophenyl)-3-propynoyl-thiazolidine-4-carboxylic acid ethyl ester (3g)

$C_{16}H_{14}N_2O_3S$

M_W = 314.36 g.mol^{-1}

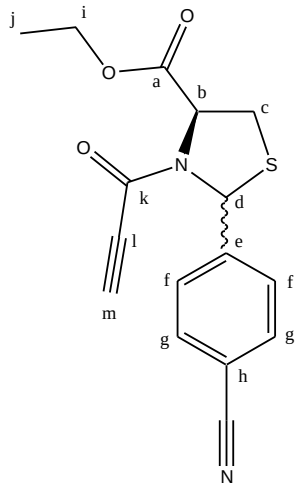

Yield: 24% (Yellow oil, 74 mg), R_f: 0.70 ethyl acetate:*n*-hexane (30:70)

^{1}H NMR ($CDCl_3$) δ: 1.32 (t, *J*= 7.2 Hz, 3H, H_j); 3.10 (s, 0.5H, H_m); 3.13 (s, 0.5H, H_m); 3.14 (dd, J_1=1.6 Hz, J_2= 10.4 Hz, 0.5H, H_c); 3.38 (dd, J_1= 7.2 Hz, J_2= 10.4 Hz, 1H, H_c); 3.49 (dd, J_1= 7.2 Hz, J_2= 10.4 Hz, 0.5H, H_c); 4.04 (t, *J*= 6.8 Hz, 1H, H_b); 4.24-4.31 (m, 2H, H_i); 5.58 (s, 0.5H, H_d); 5.87 (s, 0.5H, H_d); 7.58-7.69 (m, 4H, H_f + H_g).

(2*RS*,4*R*)-2-Pentyl-3-propynoyl-thiazolidine-4-carboxylic acid ethyl ester (3h)

$C_{14}H_{21}NO_3S$

Mw: 283.39 g.mol^{-1}

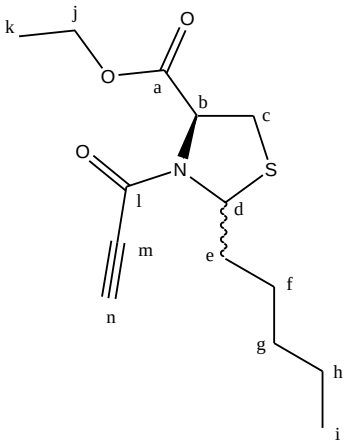

Yield: 55% (Yellow oil, 138 mg), R_f: 0.73 ethyl acetate:*n*-hexane (30:70)

^{1}H NMR ($CDCl_3$) δ: 0.86-0.92 (m, 3H, H_i); 1.25-1.34 (m, 9H, H_k + H_f + H_g + H_h); 1.77-1.81 (m, 1H, H_c); 2.10-2.12 (m, 1H, H_c); 3.06 (s, 0.4H, H_n); 3.17 (s, 0.6H, H_n); 3.30-3.39 (m, 2H, H_e); 4.25 (m, 2H, H_j); 4.96 (t, *J*=8.0 Hz, 0.6H, H_b); 5.15 (dd, J_1= 4.8 Hz, J_2= 6.8 Hz, 0.4H, H_b); 5.31-5.36 (m, 1H, H_d).

FT-IR (KBr), cm^{-1}: 3251 (C-H, C≡C-H), 2112 (C≡C), 1739 (C=O, ester), 1634 (C=C, aromatic).

(2*RS*,4*R*)-2-Butyl-3-propynoyl-thiazolidine-4-carboxylic acid ethyl ester (3i)

$C_{13}H_{19}NO_3S$

Mw: 269.36 g.mol^{-1}

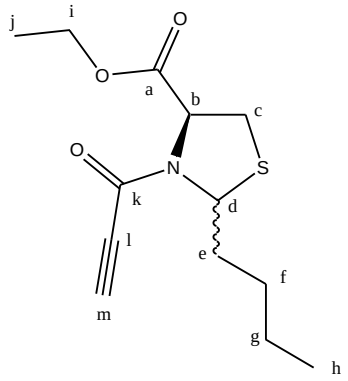

Yield: 87% (Yellow oil, 122 mg), R_f: 0.74 ethyl acetate:*n*-hexane (30:70)

^{1}H NMR ($CDCl_3$) δ: 0.88-0.95 (m, 3H, H_h); 1.25-1.62 (m, 7H, H_f + H_g + H_j); 1.78-1.83 (m, 1H, H_e); 2.10-2.21 (m, 1H, H_e); 3.07 (s, 0.4H, H_m); 3.17 (s, 0.6H, H_m); 3.29-3.40 (m, 2H, H_c); 4.18-4.30 (m, 2H, H_i); 4.96 (t, *J*=8.0 Hz, 0.6H, H_b); 5.15 (dd, J_1= 6.0 Hz, J_2= 7.2 Hz, 0.4H, H_b); 5.33 (td, J_1= 4.4 Hz, J_2= 9.6 Hz, 1H, H_d).

^{13}C NMR (DMSO-d_6) δ: 13.9, 13.9 (C_h); 14.0, 14.1 (C_j); 22.0, 22.2 (C_g); 29.0, 29.0 (C_f); 32.1, 32.7 (C_e); 35.6, 37.5 (C_c); 61.5, 61.9 (C_i); 62.2, 64.2 (C_b); 64.3, 66.5 (C_d); 75.7, 76.0 (C_m); 78.4, 79.1 (C_l); 150.7, 151.1 (C_k); 169.5, 169.8 (C_a).

FT-IR (KBr), cm^{-1}: 3242 (C-H, C≡C-H), 2107 (C≡C), 1746 (C=O, ester), 1634 (C=C, aromatic).

LC – MS: ELSD, rt = 4.37 min., *m*/*z* 270 $[M + H]^+$, 311 $[M + CH_3CN]^+$.333 $[M + CH_3CN + Na]^+$.

(2*RS*,4*R*)-2-(1-Ethylpentyl)-3-propynoyl-thiazolidine-4-carboxylic acid ethyl ester (3j)

$C_{16}H_{25}NO_3S$

Mw= 311.44 g.mol^{-1}

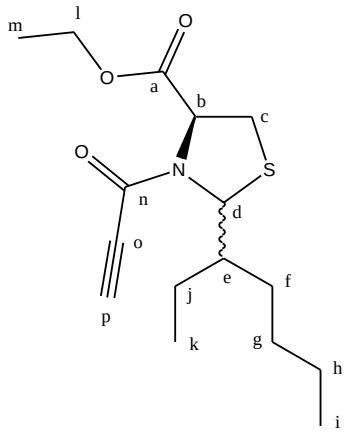

Yield: 30% (Yellow oil, 75 mg), R_f: 0.72 ethyl acetate:*n*-hexane (30:70)

^{1}H NMR ($CDCl_3$) δ: 0.85-0.97 (m, 6H, H_i + H_k); 1.26-1.82 (m, 12H, H_e + H_f + H_g + H_h + H_m); 3.10 (s, 0.4H, H_p); 3.20 (s, 0.6H, H_p); 3.33 (m, 2H, H_c); 4.19-4.29 (m, 2H, H_l); 4.97 (q, *J*= 8.0 Hz, 0.6H, H_b); 5.14 (td, J_1= 2.4 Hz; J_2= 4.0 Hz, 0.4H, H_b); 5.39 (dd, J_1= 4.0 Hz; J_2= 8.4 Hz, 0.6H, H_d); 5.45 (dd, J_1= 2.4 Hz; J_2= 8.4 Hz, 0.4H, H_d).

LC – MS: ELSD, rt = 5.37 min., *m*/*z* 312 $[M + H]^+$, 353 $[M + CH_3CN]^+$, 375 $[M + CH_3CN + Na]^+$.

(2*RS*, 4*R*)-2-(2,4,4-Trimethylpentyl)-3-propynoyl-thiazolidine-4-carboxylic acid ethyl ester (3k)

$C_{17}H_{27}NO_3S$

Mw: 325.17 g.mol^{-1}

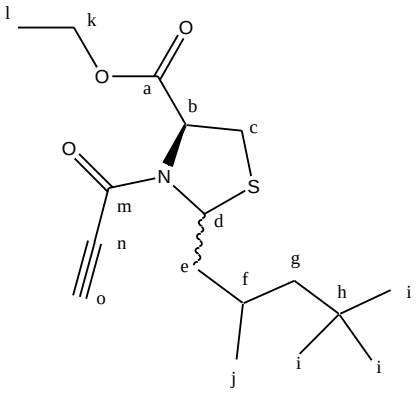

Yield: 55% (Yellow oil, 193 mg) R_f: 0.76 ethyl acetate:*n*-hexane (30:70)

^{1}H NMR ($CDCl_3$) δ: 0.90 (s, 9H, H_i); 0.98 (d, *J*=6.8 Hz, 1.8H, H_j); 1.02 (d, *J*=6.4 Hz, 1.2H, H_j); 1.25-1.31 (m, 3H, H_l); 1.39-1.94 (m, 5H, H_e + H_f + H_g); 2.88 (s, 0.4H, H_o); 3.05 (s, 0.6H, H_o); 3.17 (d, *J*= 5.6 Hz, 0.6H, H_c), 3.24-3.40 (m, 1.4H, H_c); 4.18-4.29 (m, 2H, H_k); 4.94 (td, J_1= 2.8 Hz, J_2= 8.0 Hz, 0.6H, H_b); 5.15 (t, *J*= 8.0 Hz, 0.4H, H_b); 5.34-5.43 (m, 1H, H_d).

FT-IR (KBr), cm^{-1}: 3243 (C-H, C≡C-H), 2109 (C≡C), 1743 (C=O, ester), 1634 (C=C, aromatic).

(2*RS*,4*R*)-2-(1-Methylbutyl)-3-propynoyl-thiazolidine-4-carboxylic acid ethyl ester (3l)

$C_{14}H_{21}NO_3S$

Mw= 283.39 g.mol^{-1}

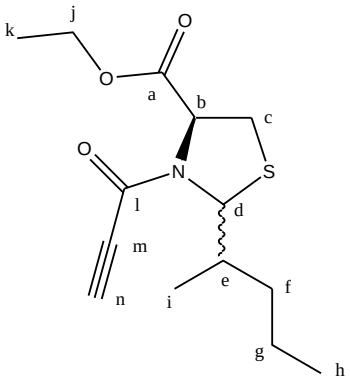

Yield: 63% (Yellow oil, 157 mg), R_f: 0.75 ethyl acetate:*n*-hexane (30:70)

^{1}H NMR ($CDCl_3$) δ: 0.88-0.97 (m, 3H, H_h); 1.04 (d, *J*= 6.4 Hz, 1.2H, H_i); 1.15 (d, *J*= 6.4 Hz, 1.8H, H_i); 1.22-1.33 (m, 5H, H_e + H_f + H_g); 1.42-1.80 (m, 3H, H_k); 3.11 (d, *J*= 4.0 Hz, 0.4H, H_n); 3.18 (d, *J*= 4.0 Hz, 0.6H, H_n); 3.25-3.39 (m, 2H, H_c); 4.18-4.30 (m, 2H, H_j); 4.92 (t, *J*= 8.0 Hz, 0.4H, H_b); 5.00 (t, *J*= 8.0 Hz, 0.6H, H_b); 5.10-5.30 (m, 1H, H_d).

FT-IR (KBr), cm^{-1}: 3243 (C-H, C≡C-H), 2107 (C≡C), 1634 (C=C, aromatic).

LC – MS: ELSD, rt = 6.32 min., *m*/*z* 284 $[M + H]^+$, 325 $[M + CH_3CN]^+$, 347 $[M + CH_3CN + Na]^+$.

(2*RS*,4*R*)-2-tert-Butyl-3-propynoyl-thiazolidine-4-carboxylic acid ethyl ester (3m)

$C_{13}H_{19}NO_3S$

Mw= 269.36 g.mol^{-1}

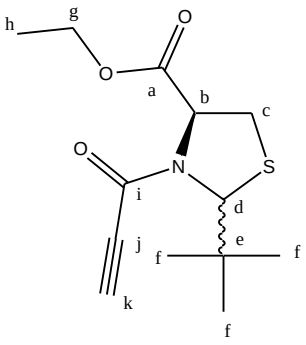

Yield: 52% (Yellow oil, 100 mg), R_f: 0.76 ethyl acetate:*n*-hexane (30:70)

^{1}H NMR ($CDCl_3$) δ: 1.03 (s, 4.5H, H_f); 1.10 (s, 4.5H, H_f); 1.29 (t, *J*= 6.8 Hz, 1.5H, H_h); 1.32 (t, *J*= 6.8 Hz, 1.5H, H_h); 3.12 (s, 0.5H, H_k); 3.23 (s, 0.5H, H_k); 3.39-3.47 (m, 2H, H_c); 4.21-4.29 (m, 2H, H_g); 5.02 (t, *J*= 9.2 Hz, 0.5H, H_b); 5.13 (t, *J*= 8.8 Hz, 0.5H, H_b); 5.33 (s, 0.5H, H_d); 5.39 (s, 0.5H, H_d).

FT-IR (KBr), cm^{-1}: 3233 (C-H, C≡C-H), 2108 (C≡C), 1740 (C=O, ester), 1626 (C=C, aromatic).

LC – MS: ELSD, rt = 5.99 min., *m*/*z* 270 $[M + H]^+$, 333 $[M + CH_3CN + Na]^+$.

5 RESULTS AND DISCUSSION

This study consisted of the generation of novel (*2RS,4R*)-3-propionyl-thiazolidine-4-carboxylic acid ethyl ester derivatives as analogues of the cytotoxic ALC67 molecule in order to analyze the impact of the phenyl moiety that presents at the second position of the thiazolidine ring on the antiproliferative property of the molecule.

5.1 Chemistry

The retrosynthetic route that led to the formation of the ALC67 analogues is given below (Scheme 5). The final compounds (**3a-3m**) that were targeted to be obtained present three main moieties: a thiazolidine ring, an ethyl ester and a propionyl group. The propionyl group was thought to be introduced by the acylation of the secondary amine of the thiazolidine system which contains a carboxylic acid ester at 4th position (**2a-2m**) in the presence of propiolic acid and (**2a-2m)** compounds obtained by the reaction of (**1a-1m)** with ethanol esterification. Then 4-carboxylic acid function of the thiazolidine (**1a-1m)** that could be generated from the classical reaction of *L*-cysteine with appropriate aldehyde.

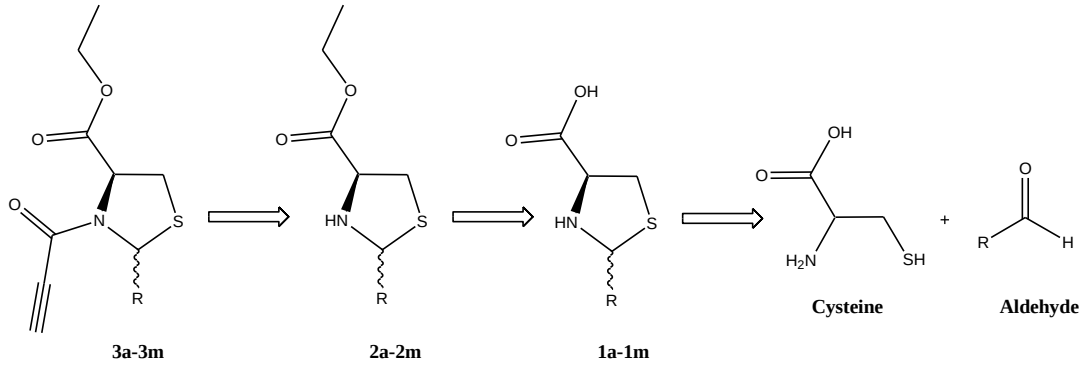

Scheme 5. Retrosynthesis of (2RS,4R) 3-propionyl-thiazolidine-4-carboxylic acid ethyl ester

5.1.1 Generation of the thiazolidine cycle: synthesis of 1a-1m

The first step consisted of the generation of the thiazolidine ring from the nucleophilic addition reaction of *L*-cysteine (aminothiol) on a series of commercial aliphatic and aromatic aldehydes. The reaction was conducted in basic conditions, thus should have proceeded through a Schiff base intermediate, following the mechanism shown in scheme 6. As the ring-closure generates a new chiral center in an uncontrolled manner as already mentioned in section 2.2.1, thiazolidine compounds are obtained as diastereomeric mixtures.

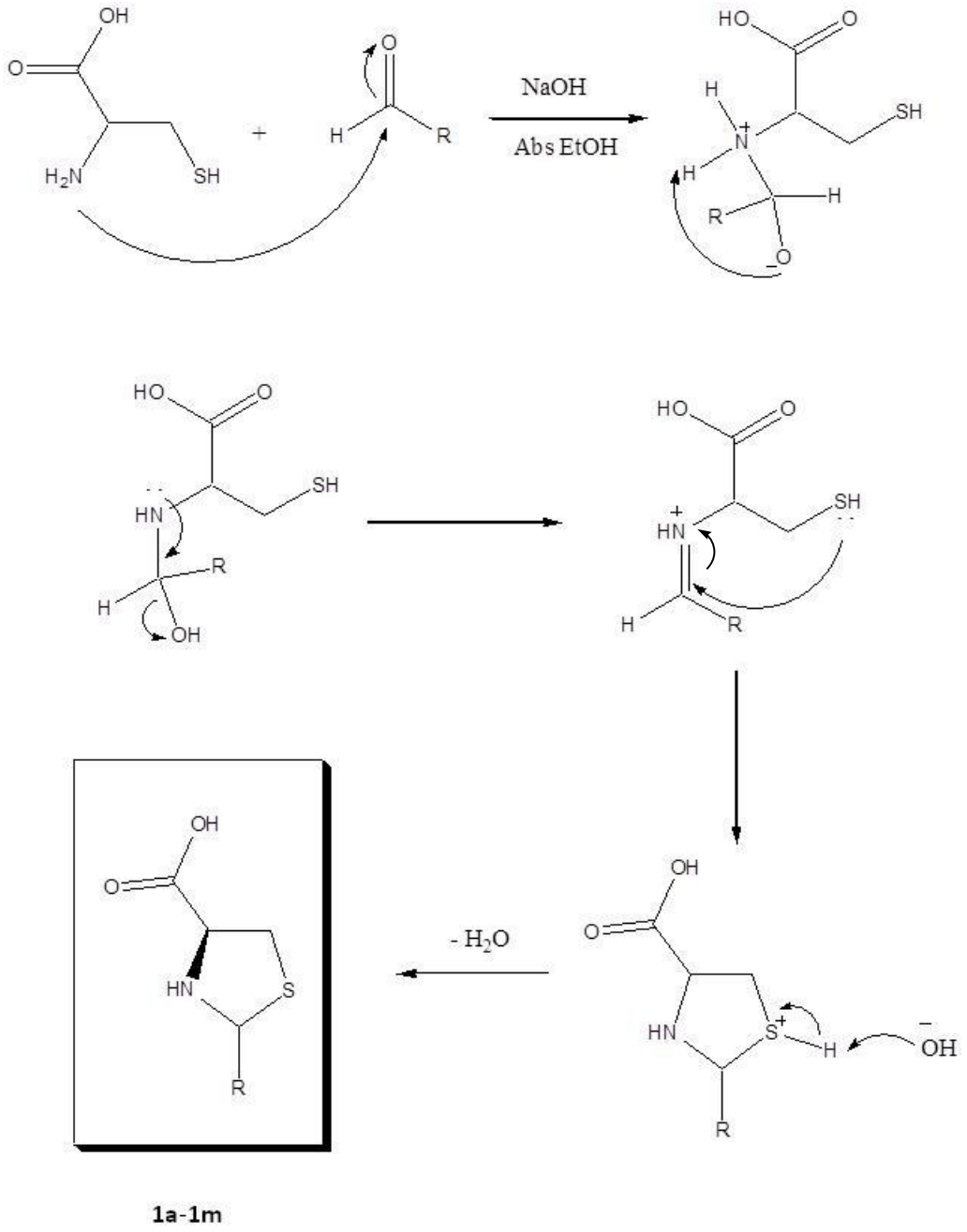

Scheme 6. Cyclisation of *L*-cysteine in basic conditions.

Thiazolidine formation is an easy and efficient reaction that gives the expected products with satisfactory yields (Table 4).

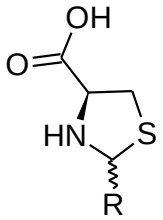

R		Yield (%)
p-OCH_3-Ph-	(**1a**)	66
p-F-Ph-	(**1b**)	65
m-F-Ph-	(**1c**)	74
o-F-Ph-	(**1d**)	73
p-HO-Ph-	(**1e**)	70
p-CN-Ph-	(**1g**)	63
-$(CH_2)_4CH_3$	(**1h**)	90
-$(CH_2)_5CH_3$	(**1i**)	36
-$CH(CH_2\text{-}CH_3)\text{-}CH_2CH_2CH_2CH_3$	(**1j**)	92
-$CH_2\text{-}CH(CH_3)\text{-}CH_2\text{-}C(CH_3)_3$	(**1k**)	80
-$CH(CH_3)\text{-}CH_2CH_2CH_3$	(**1l**)	61
-$C(CH_3)_3$	(**1m**)	59

Table 4. Yields of (*2RS,4R*)-2-Phenylthiazolidine-4-carboxylic acids **1a-1m**

Synthesized carboxylic acid molecules were analyzed by FT-IR, ^{1}H NMR, ^{13}C NMR and mass spectrometry. The generation of the heterocyclic structure was confirmed with ^{1}H NMR since spectra exhibited the expected characteristic signals of a thiazolidine cycle. Indeed, in addition to the singlets at around 5.2 and 5.6 ppm that correspond to the signals of C2-H of each diastereomer, a pair of dd at around 4.2 and 3.80 for the C4-H and a set of four dd around 3.3 ppm for the unequivalent C5-Hs were also recorded on spectra (see p.8 for more information on signal attribution). The successful formation of the thiazolidine ring was also validated by ^{13}C NMR as spectra displayed the typical signals of C2, C4 and C5 of the ring at around 71, 65 and 38 ppm respectively.

The 2R, 4R and 2S, 4R diastereomers were obtained in general in a 40:60 ratio. This ratio was easily determined using the C2-H singlet signals of ^{1}H NMR. Interestingly the thiazolidines deriving from *o*-fluorobenzaldehyde and trimethylacetaldehyde (**1d** and **1m** respectively) gave diastereomers in a 15:85 and 5:95 ratios, probably due to the steric hinderance caused by the proximity of the fluorous atom or the *tert*-butyl group to the carboxylic acid moiety in the *2R, 4R* configuration.

Moreover, **1k** and **1l** were prepared from racemic mixtures of 3,5,5-trimethylhexanal and 2-methylpentanal respectively. That is why each aldehyde led to four different thiazolidines: the ^{1}H NMR spectra of these compounds exhibited four different doublets for the C2-H and the ^{13}C NMR showed sets of four peaks for each signal (Figure 17).

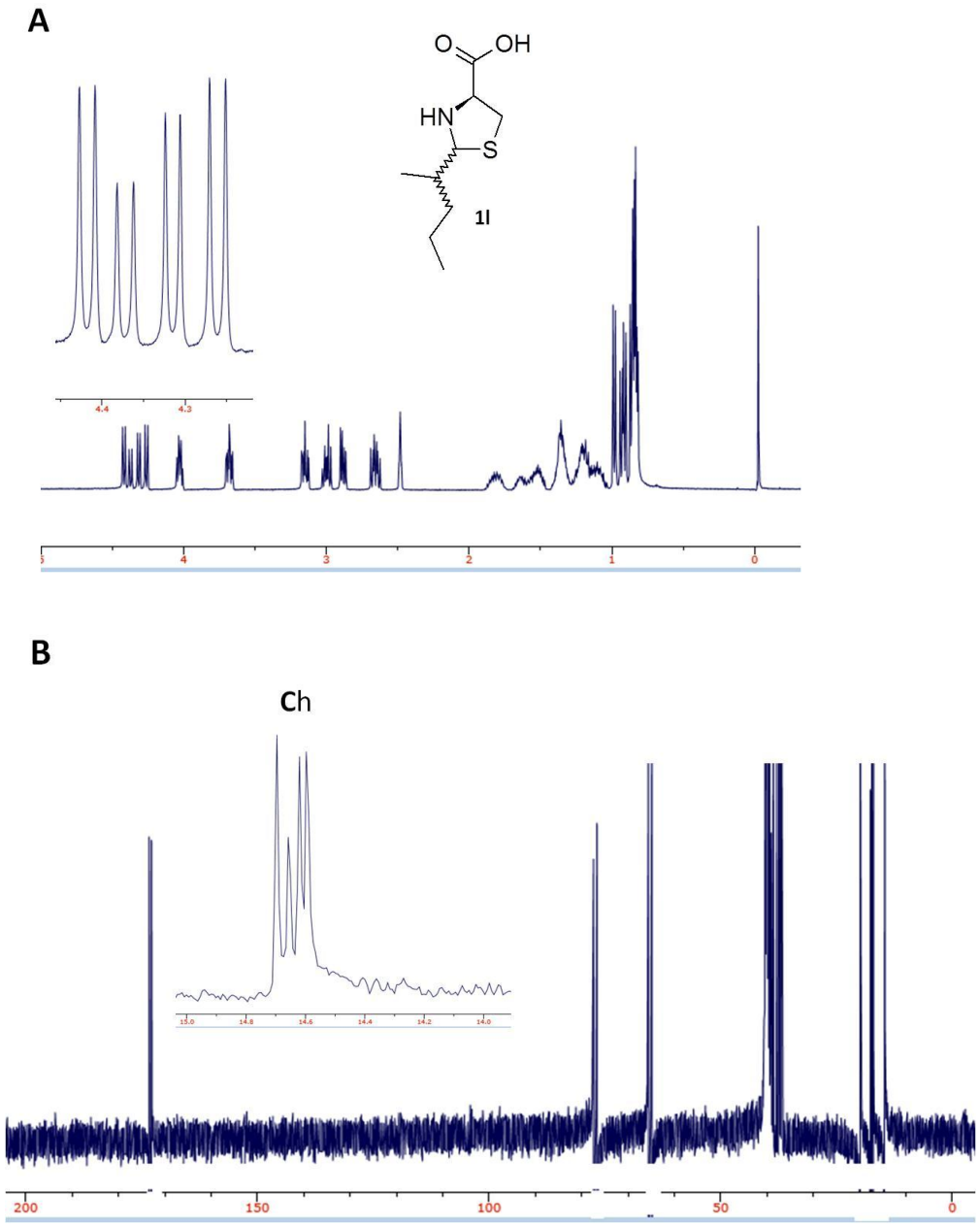

Figure 17. A. ^{1}H NMR of **1l**, B. ^{13}C NMR of **1l**

Given the difficulty of separation, the isomers were not isolated neither when proceeded to the esterification or acylation steps, nor when biologically evaluated.

5.1.2 The esterification step: Synthesis of 2a-2m

Conversion of carboxylic acid derivatives into ethyl ester moieties was realized in the presence of thionyl chloride in absolute ethanol according to the reaction mechanism shown in scheme 7.

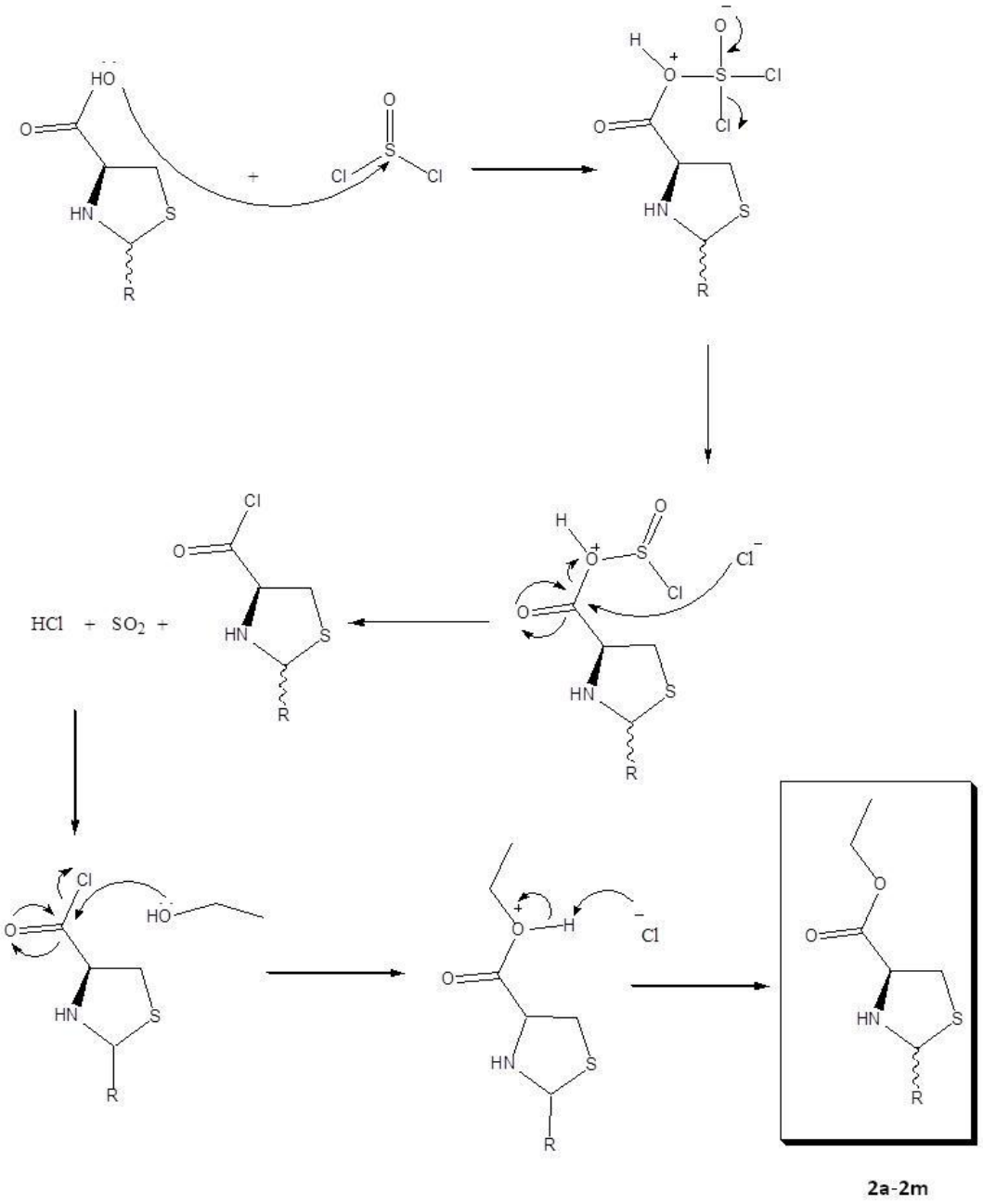

Scheme 7. Reaction mechanism of the conversion of carboxylic acid derivatives into ethyl esters.

The generation of the ethyl ester function was readily confirmed by FT-IR since the typical large band at around 3300 cm-1 corresponding the hydroxyl of the carboxylic acid function was no longer detected (Figure 18).

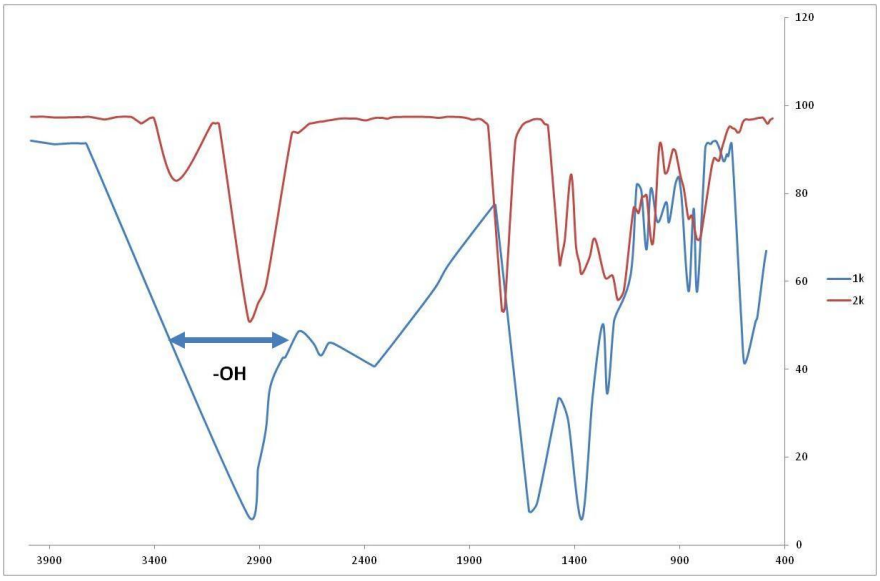

Figure 18. FT-IR spectra of **1k** and **2k**

NMR analyses were not performed on these molecules because of an instability of molecules. In fact, after treatment though pure compounds were obtained (checked on TLC), they were shown to decompose when stored (Figure 19).

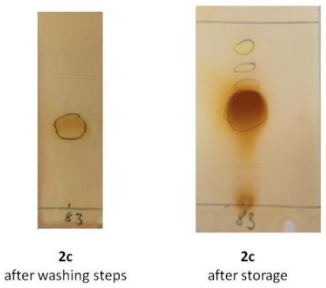

Figure 19. Decomposition of ethyl ester derivatives with time

This is why all obtained ester derivatives were directly acylated without further analyses.

5.1.3 Acylation of the heterocyclic secondary amine: Synthesis of 3a-3m

In order to get ALC67 analogues (**3a-3m**) a propionyl group was introduced to the secondary amine of the thiazolidine ring of **2a-2m** molecules. The peptidic coupling reaction was carried out by activating classically the carboxylic acid function of propiolic acid by DCC. The mechanism of the reaction in such conditions is depicted in scheme 8.

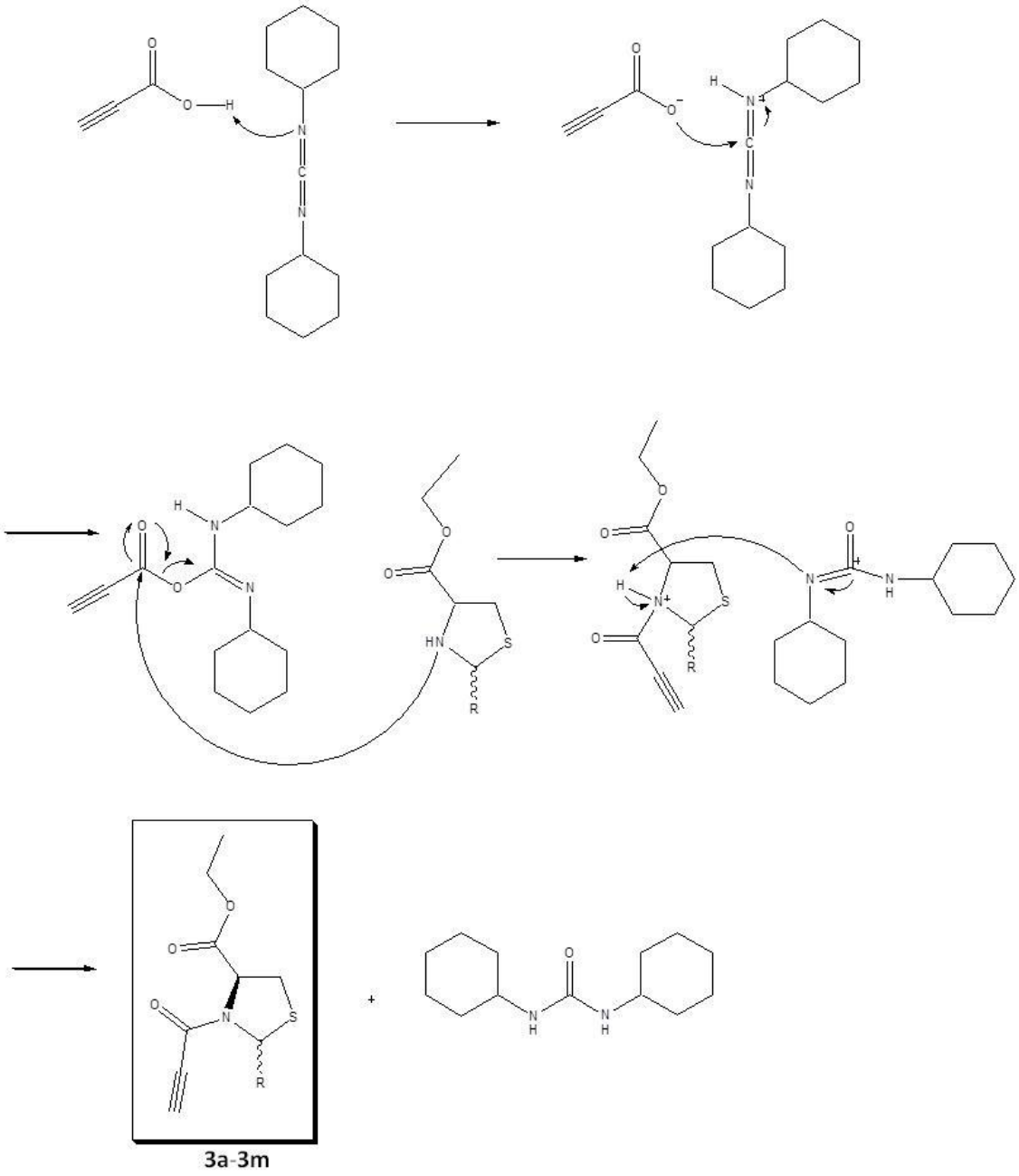

Scheme 8. Mechanism of the DCC activated peptidic coupling reaction.

The presence of the terminal alkyne was analyzed by FT-IR, ^{1}H NMR and ^{13}C NMR. In fact the infrared spectra gave in addition to the band at 2100 cm^{-1} that corresponds to the stretching band of the **C≡C** bond, a strong and narrow band at 3200 cm^{-1} for the **H-C**≡C stretching (Figure 20).

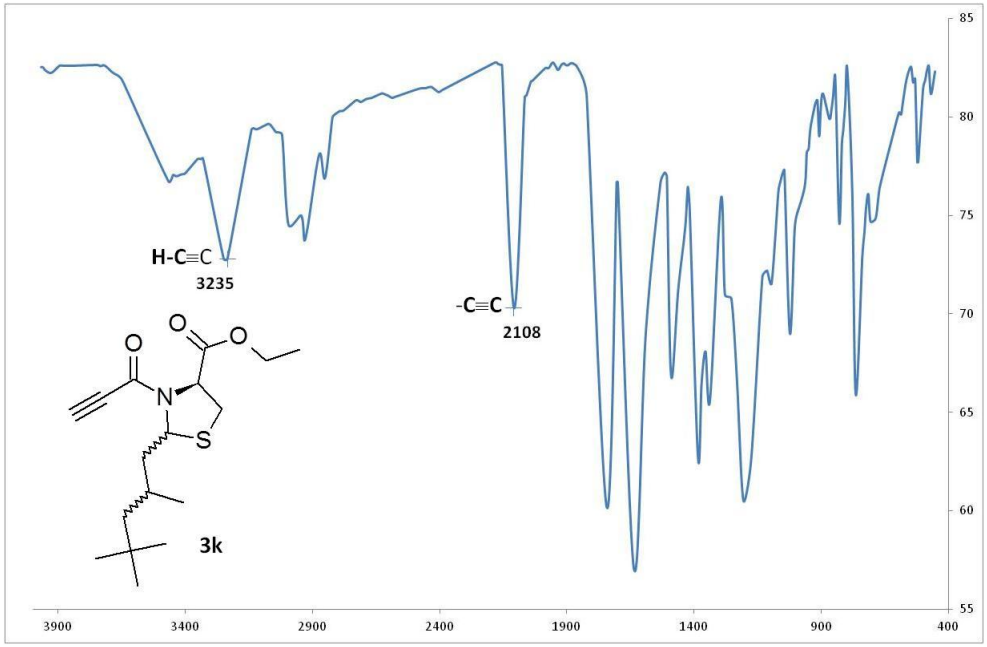

Figure 20. FT-IR spectrum of 3k depicting the characteristic bands of the terminal alkyne function

The presence of two singlets around 3.25 ppm that are typical of terminal alkyne protons on ^{1}H NMR and peaks of sp hybridized carbons observed around 75 and 81 ppm on ^{13}C NMR also confirmed the successful synthesis of **3a**-**3m** molecules (except **3e** and **3f** for which synthesis was not achieved)(Figure 21).

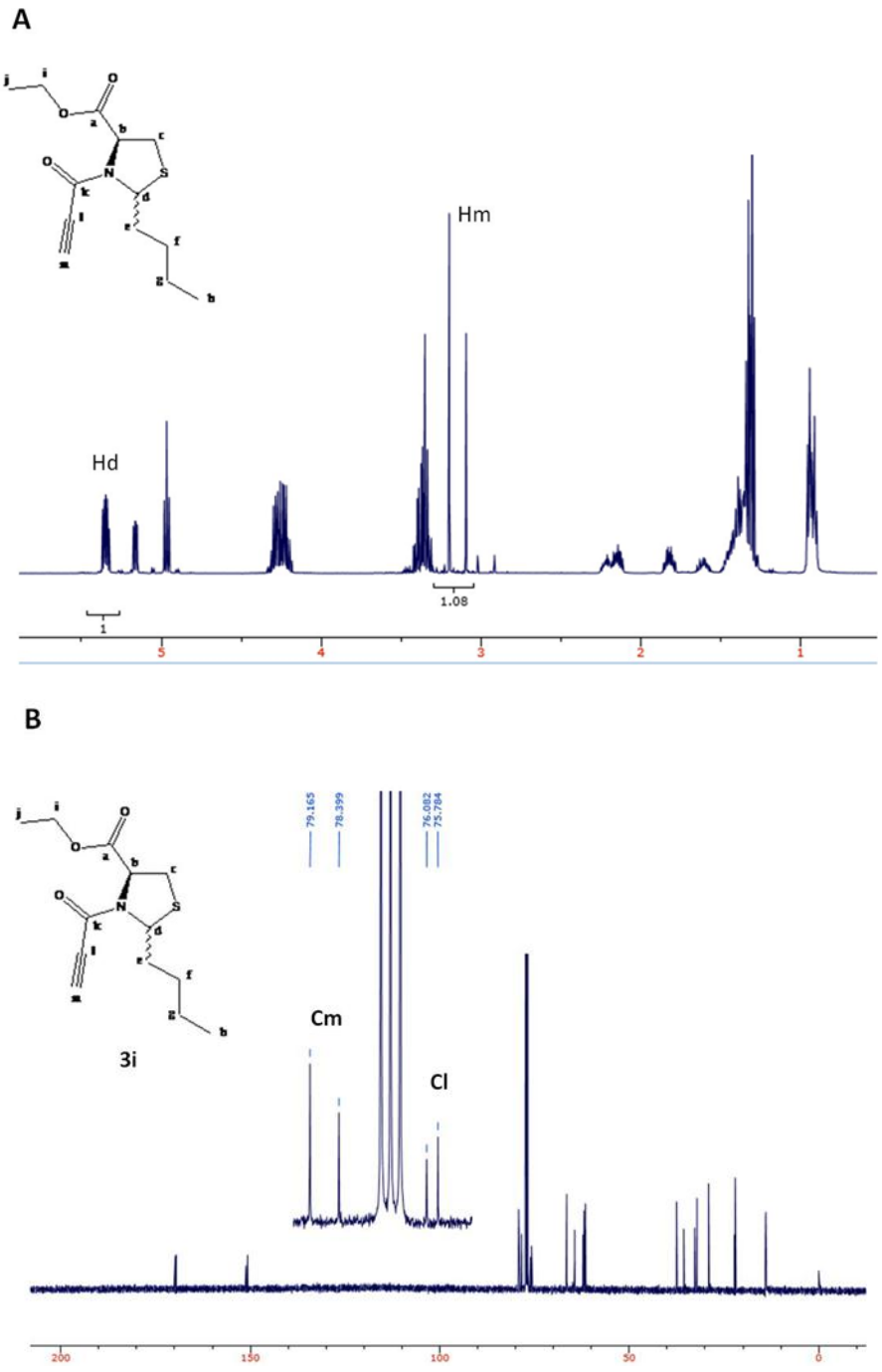

Figure 21. NMR spectra of **3i** exhibiting characteristic peaks of the terminal alkyne function

Yields for these compounds **3a- 3m** are given in table 5.

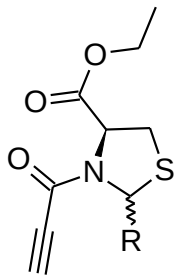

R		Yield (%)
p-OCH_3-Ph-	(**3a**)	89
p-F-Ph-	(**3b**)	37
m-F-Ph-	(**3c**)	58
o-F-Ph-	(**3d**)	30
p-CN-Ph-	(**3g**)	24
-$(CH_2)_4CH_3$	(**3h**)	55
-$(CH_2)_5CH_3$	(**3i**)	87
-$CH(CH_2\text{-}CH_3)\text{-}CH_2CH_2CH_2CH_3$	(**3j**)	30
-$CH_2\text{-}CH(CH_3)\text{-}CH_2\text{-}C(CH_3)_3$	(**3k**)	55
-$CH(CH_3)\text{-}CH_2CH_2CH_3$	(**3l**)	63
-$C(CH_3)_3$	(**3m**)	52

Table 5. Yields of **3a-3m.**

5.2 Biology

The antiproliferative activity of alkyne compounds (**3a-3m**) was examined on two different hepatocellular carcinoma cell lines (HUH7 and Mahlavu) using the sulforhodamine B assay. The obtained cytotoxicity was compared to the activity of ALC67, campthotecin and 5-fluorouracil.

Modifications that were carried out on the 2nd position did not change significantly the activity of ALC67 since all obtained IC_{50} values are similar to ALC67's (Table 6): the bioactivity of the terminal alkyne molecule was kept when the phenyl moiety was replaced either by aliphatic or aromatic groups suggesting that this position is not essential for the molecule to be cytotoxic.

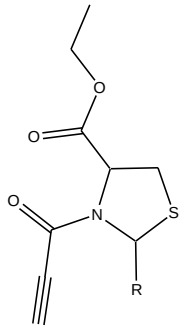

R		Huh7 IC_{50} µM	MV IC_{50} µM
ALC 67		5.3 ± 0.9	0.4 ± 0.5
p -OCH_3-Ph-	(**3a**)	1.4 ± 0.1	0.7 ± 0.2
p -F-Ph-	(**3b**)	0.7 ± 0.2	0.4 ± 0.2
m -F-Ph-	(**3c**)	1.4 ± 0.4	1.7 ± 2.0
o -F-Ph-	(**3d**)	1.7 ± 0.4	1.7 ± 0.6
p -CN-Ph-	(**3g**)	2.6 ± 0.6	2.4 ± 2.3
-$(CH_2)_4CH_3$	(**3h**)	1.8 ± 0.4	2.0 ± 1.4
-$(CH2)_3CH_3$	(**3i**)	0.5 ± 0.1	0.4 ± 0.1
-$CH(CH_2$-$CH_3)$-$CH_2CH_2CH_2CH_3$	(**3j**)	1.7 ± 0.3	1.6 ± 0.2
-CH_2-$CH(CH_3)$-CH_2-$C(CH_3)_3$	(**3k**)	1.6 ± 0.4	1.1 ± 0.6
-$CH(CH_3)$-CH_2-CH_2CH_3	(**3l**)	0.6 ± 0.3	0.5 ± 0.1
-$C(CH_3)_3$	(**3m**)	0.8 ± 0.1	0.9 ± 0.1
CPT		0.1	<1
5FU		30.7	10.0

Table 6. IC_{50} values of ALC67 analogues on HUH7 and Mahlavu (MV) hepatocellular carcinoma cell lines determined by the SRB assay.

The effect of the substitution of the phenyl moiety was analyzed through the **3a**-**3d**, and **3g** compounds. The activity did not vary according to the electron donor or acceptor property of the pending group: with the *para*-substituted molecules (**3a**, **3b** and **3g**), the best activity was observed for the *para*-fluorophenyl substituted derivative (smallest IC_{50} value, 0.7 and 0.4µM on HUH7 and MV respectively) while the electron donating methoxy and the electron attracting cyano substitutions led to greater IC_{50} values (1.4 and 2.6µM respectively on HUH7 and 0.7 and 2.4µM on MV cell lines).

Also, to investigate the effect of the substitution position we prepared the *ortho*- (**3d**), *meta*- (**3c**) and *para*-fluoro phenyl (**3b**) analogues. Results revealed a better activity for the *para*-fluorophenyl compound indicating a possible impact of the position of substitution on the biological activity possibly due to the generated steric hinderance.

Regarding the thiazolidines deriving from alkyl aldehydes, the determined IC_{50} values show that the biological activity is maintained with both linear (**3h**, **3i**) and branched chains (**3j**-**3m**), the best activity being noticed for the **3i** molecule.

All these results demonstrate that the phenyl moiety present on the 2nd position of the thiazolidine ring is not crucial for the activity to be maintained, allowing the rapid and easy preparation of similarly cytotoxic novel molecules.

6 CONCLUSION

In conclusion, in this study a series of novel cytotoxic thiazolidine molecules deriving from ALC67 was developed by substituting the phenyl group that this molecule presents on its structure by aliphatic and aromatic moieties. Thirty three new molecules, eleven of which are ALC67 analogues (**3a**-**3m**) were generated. The bioactivity tests that were carried out on all active compounds indicated that variations performed on the 2nd position of the thiazolidine ring of ALC67 did not alter significantly the cytotoxicity of the molecule, and novel ALC67 derivatives (**3a**-**3m**) showed even better activity then ALC67. Consequently, activity of the ALC67 is not sensitive to modifications undertaken on this position.

The exact mechanism of action of ALC67 remains unknown and in order to elucidate it we seek to introduce, in a future study, a fluorophore tag to its structure to track it in cancer cells. Since this investigation indicated that the cytotoxic activity of the molecule resists to modifications on the second position, this location seems suitable for the further introduction of a BODIPY tag on ALC67, starting the synthesis by the generation of a fluorescent aldehyde according to the synthetic route described by Shao *et al*. (Scheme 9) (56).

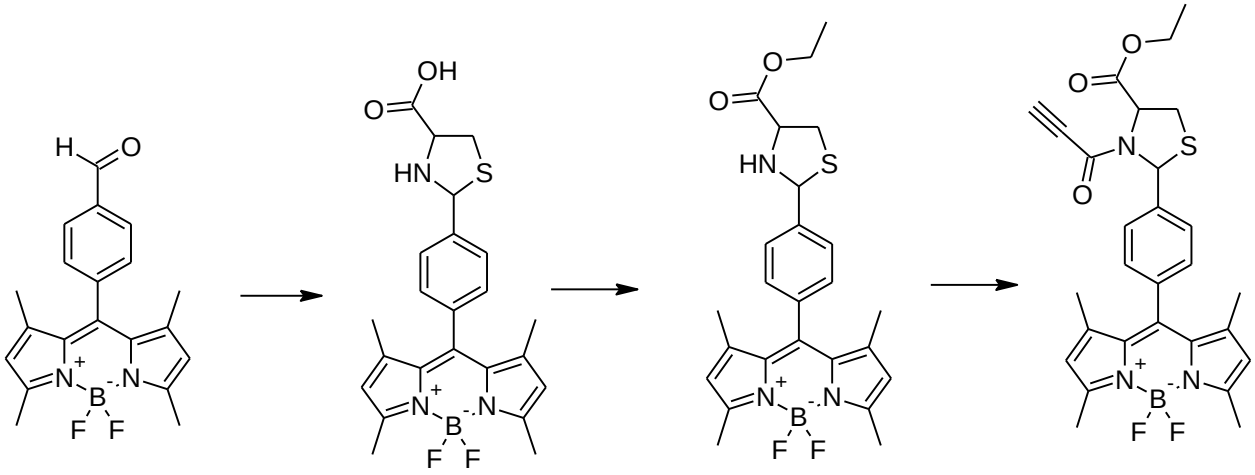

Scheme 9. Synthetic pathway for the introduction of BODIPY to ALC67

7 REFERENCES

1. Lodish H, Berk A, Matsudaira P, Kaiser AC, Krieger M, Scott PM, et al. Molecular Cell Biology. Fifth edition ed: W. H. Freeman; 2003; Gilman A. The initial clinical trial of nitrogen mustard. Am J Surg, 105: 574 - 578, 1963; Joensuu H. Systemic chemotherapy for cancer: from weapon to treatment. Lancet Oncol, 9: 304, 2008.
2. Knudson AG. Mutatıon and cancer-statıstıcal study of retınoblastoma. PNAS, 68: 820-823, 1971.
3. Hanahan D, Weinberg RA. The hallmarks of cancer. Cell, 100: 57 - 70, 2000.
4. Hanahan D, Weinberg RA. Hallmarks of Cancer: The Next Generation. Cell, 144: 646-674, 2011.
5. Fedi P, Tronick SR, Aaronson SA. Cancer Medicine. J.F. Holland RCR, D.L. Morton, E. Frei, D.W. Kufe, R.R. Weichselbaum, editor. Baltimore: Williams and Wilkins; 1997. 41-64 p.
6. Foley K, Eisenman R. Two MAD tails: what the recent knockouts of Madl and Mxil tell us about the MYC/MAX/MAD network. BBA-Rev Cancer, 1423: M37-M47, 1999.
7. Hayflick L. Mortality and immortality at the cellular level. A review. Biochemistry-Moscow, 62: 1180 - 1190, 1997.
8. Shay J, Bacchetti S. A survey of telomerase activity in human cancer. Eur J Cancer, 33: 787 - 791, 1997.
9. Hengartner MO. The biochemistry of apoptosis. Nature, 407: 770 - 776, 2000.
10. Kerr JF, Wyllie AH, Currie AR. Apoptosis: a basic biological phenomenon with wide-ranging implications in tissue kinetics. Br J Cancer, 26: 239 - 257, 1972.
11. Aggarwal BB. Signalling pathways of the TNF superfamily: A double-edged sword. Nat Rev Immunol, 3: 745 - 756, 2003.
12. Schulze-Osthoff K, Ferrari D, Los M, Wesselborg S, Peter ME. Apoptosis signaling by death receptors. Eur J Biochem, 254: 439 - 459, 1998.
13. Roos WP, Kaina B. DNA damage-induced cell death by apoptosis. Trends Mol Med, 12: 440 - 450, 2006.
14. Adjei AA. Blocking oncogenic Ras signaling for cancer therapy. J Natl Cancer I, 93: 1062 - 1074, 2001.
15. Vaupel P, Mayer A. Hypoxia in cancer: significance and impact on clinical outcome. Cancer Metast Rev, 26: 225 - 239, 2007.
16. Reed JC. Mechanisms of apoptosis. Am J Pathol,157: 1415 - 1430, 2000.
17. Grütter MG. Caspases: Key players in programmed cell death. Curr Opin Struc Biol, 10: 649 - 655, 2000.
18. Nicholson DW, Thornberry NA. Caspases: Killer proteases. Trends Biochem Sci, 22: 299 - 306, 1997.
19. Lakin ND, Jackson SP. Regulation of p53 in response to DNA damage. Oncogene, 18: 7644 - 7655, 1999.
20. Green DR, Reed JC. Mitochondria and apoptosis. Science, 281: 1309 - 1312, 1998.
21. Levine AJ. P53, the cellular gatekeeper for growth and division. Cell, 88: 323 - 331, 1997.
22. Oren M. Decision making by p53: life, death and cancer. Cell Death Differ, 10: 431 - 442, 2003.
23. Ozturk M, Ponchel F, Puisieux A, Marcais C. P53 gene in human hepatocarcinogenesis. Pathol Biol, 4: 21, 1993.

24. Ozturk M, Unsal K. P53 tumor suppressor gene - Its role in DNA damage response and cancer. Advances in DNA Damage and Repair: Oxygen Radical Effects, Cellular Protection, and Biological Consequences, 302: 371 - 376, 1999.
25. Auerbach R, Akhtar N, Lewis RL, Shinners BL. Angiogenesis assays: Problems and pitfalls. Cancer Metast Rev, 19: 167 - 172, 2000.
26. El-Kenawi AE, El-Remessy AB. Angiogenesis inhibitors in cancer therapy: mechanistic perspective on classification and treatment rationales. Brit J Pharmacol, 170: 712 - 729, 2013.
27. Otrock ZK, Mahfouz RAR, Makarm JA, Shamseddine AI. Understanding the biology of angiogenesis: Review of the most important molecular mechanisms. Blood Cell Mol Dis, 39: 212 - 220, 2007.
28. McColl BK, Stacker SA, Achen MG. Molecular regulation of the VEGF family - inducers of angiogenesis and lymphangiogenesis. Apmis, 112: 463 - 480, 2004.
29. Kelleher FC, O'Sullivan H, Smyth E, McDermott R, Viterbo A. Fibroblast growth factor receptors, developmental corruption and malignant disease. Carcinogenesis, 34: 2198-2205, 2013.
30. Presta M, Dell'Era P, Mitola S, Moroni E, Ronca R, Rusnati M. Fibroblast growth factor/fibroblast growth factor receptor system in angiogenesis. Cytokine Growth F R, 16: 159 - 178, 2005.
31. Singh RK, Gutman M, Bucana CD, Sanchez R, Llansa N, Fidler IJ. Interferon-alpha and interferon-beta down-regulate the expression of basic fibroblast growth-factor in human carcinomas. PNAS, 92: 4562 - 4566, 1995.
32. Stemmler MP. Cadherins in development and cancer. Mol Biosyst, 4: 835 - 850, 2008.
33. Luo BH, Carman CV, Springer TA. Structural basis of integrin regulation and signaling. Annu Rev Immunol, 25: 619 - 647, 2007.
34. Zamble DB, Lippard SJ. Cisplatin and dna-repair ın cancer-chemotherapy. Trends Biochem Sci, 20: 435 - 439, 1995.
35. Scagliotti GV, Selvaggi G. Antimetabolites and cancer: emerging data with a focus on antifolates. Expert Opin Ther Pat, 16: 189 - 200, 2006.
36. Kellner U, Rudolph P, Parwaresch R. Human DNA-topoisomerases - Diagnostic and therapeutic implications for cancer. Onkologie, 23: 424 - 430, 2000.
37. Rowinsky EK, Donehower RC. Drug-therapy - paclıtaxel (taxol). New Engl J Med, 332: 1004 - 1014, 1995.
38. Kallen RG. Mechanism of reactions involving Schiff base intermediates. Thiazolidine formation from L-cysteine and formaldehyde. J Am Chem Soc, 93: 6236 - 6248, 1971.
39. Lu Y, Wang Z, Li C-M, Chen J, Dalton JT, Li W, et al. Synthesis, in vitro structure–activity relationship, and in vivo studies of 2-arylthiazolidine-4-carboxylic acid amides as anticancer agents. Bioorg Med Chem, 18: 477 - 495, 2010.
40. Gududuru V, Hurh E, Dalton J, Miller D. Discovery of 2-arylthiazolidine-4-carboxylic acid amides as a new class of cytotoxic agents for prostate cancer. J Med Chem, 48: 2584 - 2588, 2005.
41. Unsal-Tan O, Ozadali K, Piskin K, Balkan A. Molecular modeling, synthesis and screening of some new 4-thiazolidinone derivatives with promising selective COX-2 inhibitory activity. Eur J Med Chem, 57: 59 - 64, 2012.
42. Look GC, Schullek JR, Holmes CP, Chinn JP, Gordon EM, Gallop MA. The identification of cyclooxygenase-1 inhibitors from 4-thiazolidinone combinatorial libraries. Bioorg Med Chem Lett, 6: 707 - 712, 1996.

43. Subbaramaiah K, Zakim D, Weksler BB, Dannenberg AJ. Inhibition of cyclooxygenase: A novel approach to cancer prevention. P Soc Exp Biol Med, 216: 201 - 210, 1997.
44. Masoud GN, Youssef AM, Khalek MMA, Wahab AEA, Labouta IM, Hazzaa AAB. Design, synthesis, and biological evaluation of new 4-thiazolidinone derivatives substituted with benzimidazole ring as potential chemotherapeutic agents. Med Chem Res, 22: 707 - 725, 2013.
45. Gududuru V, Hurh E, Durgam G, Hong S, Sardar V, Xu H, et al. Synthesis and biological evaluation of novel cytotoxic phospholipids for prostate cancer. Bioorg Med Chem Lett, 14: 4919 - 4923, 2004.
46. Daaka Y. Mitogenic action of LPA in prostate. BBA-Mol Cell Biol L, 1582: 265 - 269, 2002.
47. Qi C, Park J-H, Gibbs TC, Shirley DW, Bradshaw CD, Ella KM, et al. Lysophosphatidic acid stimulates phospholipase D activity and cell proliferation in PC-3 human prostate cancer cells. J Cell Physiol, 174: 261 - 272, 1998.
48. Gududuru V, Hurh E, Dalton J, Miller D. Synthesis and antiprofilerative activity of 2-arly-4-oxo-thiazolidin-3-yl-amides for prostate cancer. Bioorg Med Chem Lett, 14: 5289 - 5293, 2004.
49. Andres CJ, Bronson JJ, D'Andrea SV, Deshpande MS, Falk PJ, Grant-Young KA, et al. 4-Thiazolidinones: novel inhibitors of the bacterial enzyme murB. Bioorg Med Chem Lett, 10: 715 - 717, 2000.
50. Onen-Bayram FE, Durmaz I, Scherman D, Herscovici J, Cetin-Atalay R. A novel thiazolidine compound induces caspase-9 dependent apoptosis in cancer cells. Bioorg Med Chem, 20: 5094 - 5102, 2012.
51. Bertamino A, Soprano M, Musella S, Rusciano M, Sala M, Vernieri E, et al. Synthesis, in vitro, and in cell studies of a new series of [Indoline-3,2 '-thiazolidine]-based p53 modulators. J Med Chem, 56: 5407 - 5421, 2013.
52. Haupt Y, Maya R, Kazaz A, Oren M. Mdm2 promotes the rapid degradation of p53. Nature, 387: 296 - 299, 1997.
53. Brown CJ, Lain S, Verma CS, Fersht AR, Lane DP. Awakening guardian angels: drugging the p53 pathway. Nat Rev Cancer, 9: 862 - 873, 2009.
54. Chène P. Inhibiting the p53–MDM2 interaction: an important target for cancer therapy. Nat Rev Cancer, 3: 102 - 109, 2003.
55. Shangary S, Wang S. Small-Molecule Inhibitors of the MDM2-p53 Protein-Protein Interaction to Reactivate p53 Function: A novel approach for cancer therapy. Annu Rev Pharmacol, 49: 223 - 241, 2009.
56. Yue Y, Guo Y, Xu J, Shao S. A bodipy-based derivative for selective fluorescence sensing of homocysteine and cysteine. New J Chem, 35: 61 - 64, 2011.

Kerem Buran

Phone number : +90 543 847 26 36
e-mail: keremburan@gmail.com
kerem.buran@yeditepe.edu.tr
Mahmut Bey cad. 15.sok No:34/13 Şirinevler/İstanbul

EDUCATION

2011-2013	MSc, Yeditepe University, Faculty of Pharmacy, Department of Pharmaceutical Chemistry
2004-2009	BSc, Middle East Technical University (METU), Faculty of Art and Science Department of Chemistry, Ankara-Turkey
1999-2003	Adnan Menderes Anatolian High School

WORK EXPERIENCE

2011-present	Teaching assistant, Yeditepe University, Faculty of Pharmacy
2009-2011	Project assistant, ERUDESP Project, METU

LANGUAGE SKILL

English: Advanced Level

PUBLICATIONS

1- Gold (I)/Zn(II) catalyzed tandem hydroamination/annulation reaction of 4-yne-nitriles ChemComm **2010**, 46, 8032-8034

2- Sol-gel approaches for elaboration of polyol dehydrogenase-based bioelectrodes Z. Phys. Chem. **2013**, 227, 667-689